

# Near threshold $J/\psi$ photoproduction and study of LHCb pentaquarks with CLAS12

M. Battaglieri\*, A. Celentano\*, and R. De Vita\*

*INFN, Sezione di Genova, 16146 Genova, Italy*

N. Baltzell, V. Burkert, V. Kubarovsky\*, and S. Stepanyan\*<sup>†</sup>

*Thomas Jefferson National Accelerator Facility, Newport News, VA 23606*

R. Paremuzyan

*University of New Hampshire, Durham, New Hampshire 03824-3568*

C. Hyde and J. Newton

*Old Dominion University, Norfolk, VA 23529*

P. Nadel-Turonski

*Stony Brook University, Stony Brook, NY 11794*

B. McKinnon

*University of Glasgow, Glasgow G12 8QQ, United Kingdom*

L. Guo

*Florida International University, Miami, FL 33199*

(Dated: May 15, 2017)

The experimental study of the  $J/\psi$  photoproduction near threshold is an attractive subject for studying the nucleon gluonic form-factor and, as has been shown recently, is a direct way to produce and study hidden-charm pentaquark states claimed by LHCb,  $P_c(4380)$  and  $P_c(4450)$ . The two approved CLAS12 experiments, E12-12-001 and E12-11-005, will be able to observe the two pentaquarks in (very) low  $Q^2$  electroproduction. Here we propose to study  $P_c(4380)$  and  $P_c(4450)$  states and extend the study of  $J/\psi$  photoproduction near the threshold using the same settings of these two approved experiments.

The E12-12-001 will measure pentaquark states detecting the same final state as for the proposed  $J/\psi$  photoproduction studies,  $e^+e^-p$  with scattered electron escaping undetected. Pentaquarks will be searched for as resonances in the invariant mass of the final state particles. The experiment E12-11-005 will study  $J/\psi$  electroproduction on hydrogen and search for hidden-charm pentaquark states in multiple final states with scattered electron detected in the CLAS12 forward tagger (FT). With appropriate triggers for the CLAS12 DAQ system, a coincidence between an electron in the FT

---

\* co-spokesperson

<sup>†</sup> contact person

and a high momentum track(s) in the CLAS12 Forward Detector (FD), the reaction  $ep \rightarrow e'p'J/\psi$  can be studied selecting  $e'p'l^\pm$  final states (here  $l^\pm = e^\pm$  or  $\mu^\pm$ ). In these final states the  $J/\psi$  and pentaquark states will be identified in the electron-proton and electron missing mass analysis, respectively. The proposed studies of charmonium production with CLAS12 in multiple final states and different modes of reaction identification (invariant mass, missing mass) are complementary to each other and to other proposed measurements at JLAB, and will provide important validation of any physics results.

## Contents

<b>I. Introduction</b>	4
<b>II. Physics motivation</b>	5
A. $J/\psi$ photoproduction and $J/\psi$ -N scattering	5
B. LHCb pentaquarks	7
<b>III. <math>J/\psi</math> cross section and production rates</b>	11
A. Photoproduction cross section	11
B. Electroproduction cross section	12
C. Pentaquark Photoproduction Cross Section	13
<b>IV. Proposed experiment</b>	15
A. Photon flux	16
B. Untagged photoproduction	16
1. Kinematics	20
2. Mass resolutions	21
3. Estimate of the pentaquark yield	24
C. Tagged electroproduction	26
1. Kinematics	27
2. Detector response	27
3. Estimate of the pentaquark yield	31
<b>V. Trigger requirements and trigger rates</b>	33
<b>VI. Expected results</b>	36

<b>VII. Comparison with approved Jefferson Lab experiments</b>	38
<b>VIII. Summary</b>	40
<b>References</b>	40

## I. INTRODUCTION

Understanding structure of the nucleon in terms of quark and gluon degrees of freedom is one important topics of modern nuclear physics. The interaction of heavy quarkonia with hadronic matter plays important role in that endeavor. Because of the small spatial size of heavy quarkonia on the hadronic scale,  $r_{\bar{Q}Q} \ll 1$  fm, QCD operator methods can be used to describe their interactions with hadrons and external probes in controlled approximation. Heavy quarkonium production probes the local color (gluon) fields in the nucleon, and can reveal properties such as their response to momentum transfer, their spatial distribution, and their correlation with valence quarks. With available beam energy and experimental facilities photo- and electroproduction of charmed quarkonium,  $\bar{c}c$ , can be studied at Jefferson Lab. Using vector meson dominance (VMD), one can relate forward  $J/\psi$  -photoproduction to  $J/\psi$  -nucleon scattering, making the photoproduction as an important tool to study  $J/\psi$  -N interactions. The dynamics that produces the relevant gluon fields in the nucleon changes considerably between high energy and the near-threshold regions. There is a considerable amount of data on  $J/\psi$  photoproduction at high energies,  $W > 10$  GeV, in good agreement with 2-gluon exchange mechanism. There are no data for energies near the production threshold,  $E_\gamma < 11$ , where the momentum transfer to the target nucleon is large and the process can viewed as an elastic scattering of quarkonium off the nucleon. Exclusive  $J/\psi$  production near threshold thus is sensitive to the nucleon form factor providing unique information on the non-perturbative gluon fields in the nucleon.

There are already approved experiments in Halls-A [1], B [2], and C [3] for studying  $J/\psi$  photo- and electroproduction. The CLAS12 experiment E12-12-001 [2] will study  $J/\psi$  photoproduction from threshold, 8.2 GeV, to the available beam energy,  $\sim 11$  GeV, using the "untagged photoproduction" technique. The CLAS12 experiment E12-11-005 [4], MesonX, will study meson spectroscopy making use of the "tagged photoproduction" technique where electrons scattered at small angles (2.5-4.5 deg) are detected in the Forward Tagger (FT) providing a low- $Q^2$  tagged photon beam. This experiment is well suited to study the  $J/\psi$  production detecting multiple final states. Since the approval of the CLAS12 experiments, new developments revamped interest in the elastic near threshold  $J/\psi$  photoproduction. In particular LHCb announced the discovery of two hidden-charm pentaquarks [5] in the  $J/\psi + p$  decay channel,  $P_c(4380)$  and  $P_c(4450)$  with minimum quark content  $c\bar{c}uud$ . These states are in the energy range of available beams for CLAS12 and can be studied in variety of final states.

Here we propose to study the  $J/\psi$  near-threshold production using tagged photoproduction

technique of the approved experiment E12-11-005, extend studies proposed in E12-12-001 to  $J/\psi \rightarrow \mu^- \mu^-$  decay mode, and study charmed pentaquarks using tagged and untagged photoproduction with CLAS12. The proposed extensions do not require any changes to the approved running conditions of E12-11-005 and E12-12-001, and therefore can run as part of the CLAS12 Run Group A (RG-A).

The proposal is organized as follows: in Section II we present the physics motivations for the proposed studies; in Section III cross section formalism for both  $J/\psi$  and hidden-charm pentaquark photoproduction are presented; in Section IV the setup description is given with the key kinematic and experimental parameters: photon fluxes for untagged- and tagged photoproduction and the expected rates. In Section V, we describe options for CLAS12 DAQ triggers. We end the proposal with a short summary.

## II. PHYSICS MOTIVATION

Since its discovery, the  $J/\psi$  meson became a subject of intense experimental studies, in particular at  $e^+e^-$  colliders. The photo- and electroproduction of  $J/\psi$  on the nucleon has been studied mostly at large energies where production proceeds predominantly at low values of transferred momentum squared  $t$ , see for example [6]. Experiments on  $J/\psi$  photo- or electroproduction in the threshold region are scarce. There are photoproduction measurements from SLAC [7] and from Cornell [8] that do not quite agree each other at lowest energy points. Jefferson Lab with the CEBAF accelerator, a 12 GeV electron machine, is in a unique position to investigate  $J/\psi$  photo- and electroproduction in great detail from the threshold, 8.2 GeV, to the end point energies.

The study of gluonic form-factors of the proton by measuring the  $t$ -dependence of the cross section, and testing the models for  $J/\psi$  production mechanism near threshold by measuring the total cross section as a function of the total center-of-mass energy are the main goals of the E12-12-001 experiment. After the discovery of hidden-charm pentaquarks by LHCb [5], a new target has been added to the  $J/\psi$  photoproduction studies proposed in Hall-B with the CLAS12 detector, production and study of these states as  $s$ -channel resonances in photon-proton scattering with subsequent decay to  $(J/\psi p)$ .

### A. $J/\psi$ photoproduction and $J/\psi$ -N scattering

The  $J/\psi$  photoproduction near threshold provides a unique opportunity to study  $J/\psi$ -N elastic scattering at small relative velocities. In the conventional VDM framework, the elastic photoproduction of a vector meson can be related to the vector-meson nucleon scattering, see e.g. [9]:

$$\frac{d\sigma_{\gamma N \rightarrow VN}}{dt} = \mathcal{K} \frac{3\Gamma(V \rightarrow e^+e^-)}{\alpha m_V} \frac{d\sigma_{VN \rightarrow VN}}{dt}, \quad (1)$$

where  $\mathcal{K}$  is a kinematic factor,  $\Gamma$  is the partial decay width of the vector meson to  $e^+e^-$ ,  $\alpha$  and  $m_V$  are the fine structure constant and the meson mass, respectively. The physical picture of this process is shown in Fig. 1 [10]. The photon fluctuates into a  $\bar{q}q$  pair in some  $l_C$  distance before the interaction (coherence length), then the  $\bar{q}q$  pair of size  $r_\perp$  scatters off the nucleon with impact parameter  $b$ , and then forms a vector meson at some distance  $l_F$  after the scattering (formation length). In the  $J/\psi$  near-threshold photoproduction these parameters are much smaller than the

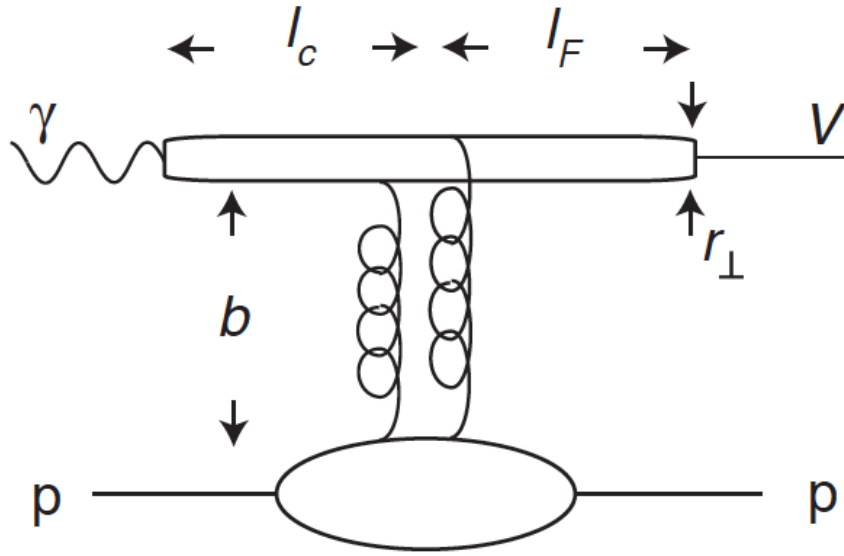


FIG. 1: VDM picture of a vector meson photoproduction (diagram is from [10]).

nucleon size:

$$\begin{aligned} l_C &= \frac{2E_\gamma}{4m_c^2} \approx 0.4 \text{ fm}, \\ b &\approx \frac{1}{\sqrt{-t}} \approx 0.2 \text{ fm}, \\ r_\perp &\approx \frac{1}{m_c} = 0.13 \text{ fm}, \\ l_F &\approx \frac{2E_{J/\psi}}{2m_c(m_{\psi'} - m_{J/\psi})} \approx 1 - 2 \text{ fm}. \end{aligned} \quad (2)$$

A small  $b$  and  $r_{\perp}$  creating conditions where the  $J/\psi$  photoproduction can be used as an effective tool to study the nucleon form factor of a gluonic operator, providing unique information on the non-perturbative gluon fields in the nucleon. In order to have an elastic scattering (where the nucleon stays intact), partons in the nucleon must share the large transferred momentum to the  $\bar{c}c$  pair and must be in a compact Fock state. The large momentum transfer can lead to the dominance of multi-gluon exchange reactions, allowing a charmonium bound state formation [11]. In Fig. 2, the analysis of the available data on energy dependence of the  $J/\psi$  photoproduction cross section by Brodsky et al. [10] is shown. As can be seen, the lowest data point from Cornell [8] (as well as few unpublished points from single arm measurements at SLAC, not shown here) do not lineup well with 2-gluon exchange curve, the red solid line on the graph. In [10] authors argue that a possible increase in the cross section close to the production threshold can be due to the 3-gluon exchange mechanism. In Ref. [12] Sibirtsev et al. proposed the exchange of an axial vector trajectory that couples with the axial form factor of the nucleon as a possible explanation for the cross section enhancement. In Ref. [13] the enhancement of the  $J/\psi$  photoproduction near threshold is explained invoking dominance of the real part of the scattering amplitude, see Fig. 3. In Ref. [14] it is shown that the real part of the amplitude contains the anomalous gluon piece of the energy-momentum tensor (conformal or trace anomaly). The latter is an important ingredient in Ji's decomposition of the proton mass [15].

## B. LHCb pentaquarks

The LHCb collaboration claimed the observation of two pentaquarks in the  $\Lambda_b^0 \rightarrow K^- P_c^+$ ,  $P_c^+ \rightarrow J/\psi p$  [5] decay channel. One state has a mass of  $4380 \pm 8 \pm 29$  MeV and a width of  $205 \pm 18 \pm 86$  MeV, while the second is narrower, with a mass of  $4449.8 \pm 1.7 \pm 2.5$  MeV and a width of  $39 \pm 5 \pm 19$  MeV. The preferred  $J^P$  assignments are of opposite parity, with one state having spin 3/2 and the other 5/2. The narrow  $P_c(4450)$  state is clearly visible in the  $J/\psi p$  invariant mass spectrum. The evidence for the other state  $P_c(4380)$  was found after rather complicated data analysis.

The decays of conventional baryons to  $J/\psi + X$  are strongly suppressed by the Okubo-Zweig-Iizuka rule. This provides a hint that these resonances contain a  $c\bar{c}$  pair and 3 light quarks in the initial state to conserve the baryonic number. In addition, the masses of these states ( $\approx 4.4$  GeV) are close to the sum of the mass  $J/\psi$  and proton. The narrow width (especially for the  $P_c(4450)$ ) supports the hypothesis that these heavy baryonic states have small probability to decay to the

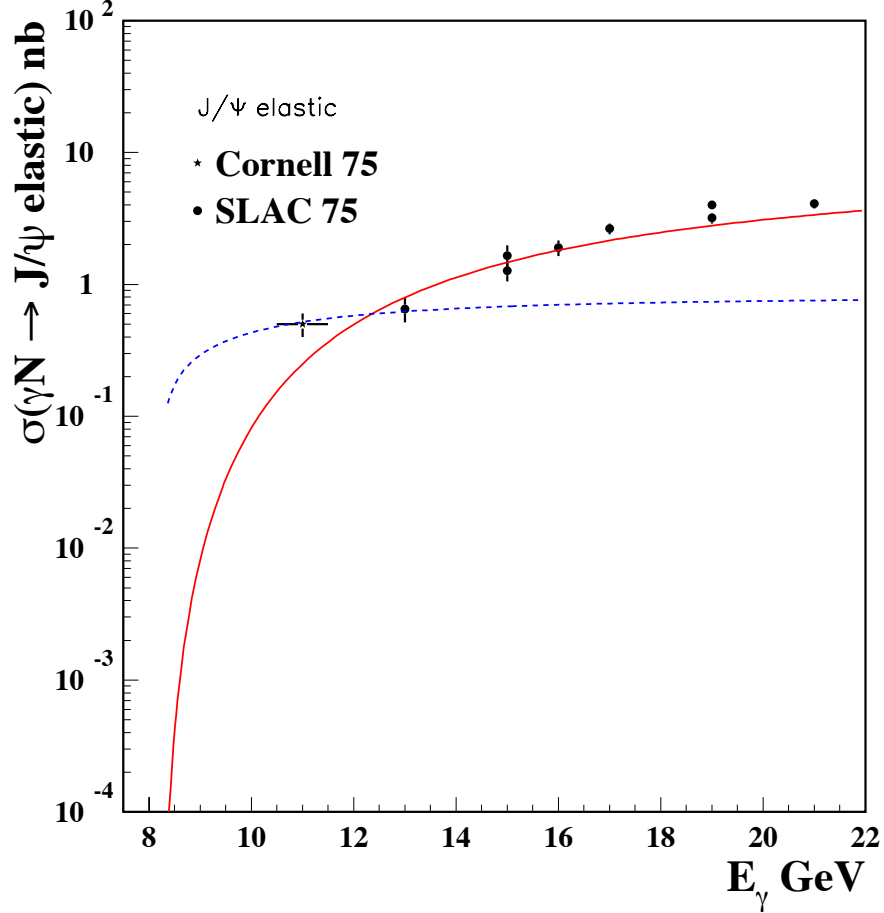


FIG. 2: Variation of the  $J/\psi$  photoproduction cross section near threshold. Solid line: two gluon exchange. Dashed line: three gluon exchange [10].

low mass mesons and baryon, which would be very difficult to explain if these states consist of the light quarks only. So the interpretation of these structures as pentaquark with hidden charm looks very reasonable.

There are several models available that attempt to describe the internal structure of the pentaquarks with hidden charm.

- The  $P_c$  states are interpreted as a composite of the charmonium state and the proton or excited nucleon states [16] similar to the known resonances  $N(1440)$  or  $N(1520)$ . In this case we expect a sizable branching ratio  $Br(P_c \rightarrow J/\psi + p)$  laying in the range from 1% to 10%. It was pointed out in [16] that in this model one can expect the decays of the pentaquarks  $P_c \rightarrow J/\psi + p + \pi$  and  $P_c \rightarrow J/\psi + p + \pi + \pi$  should at least compete in the total rate with the observed  $J/\psi + p$  channel.

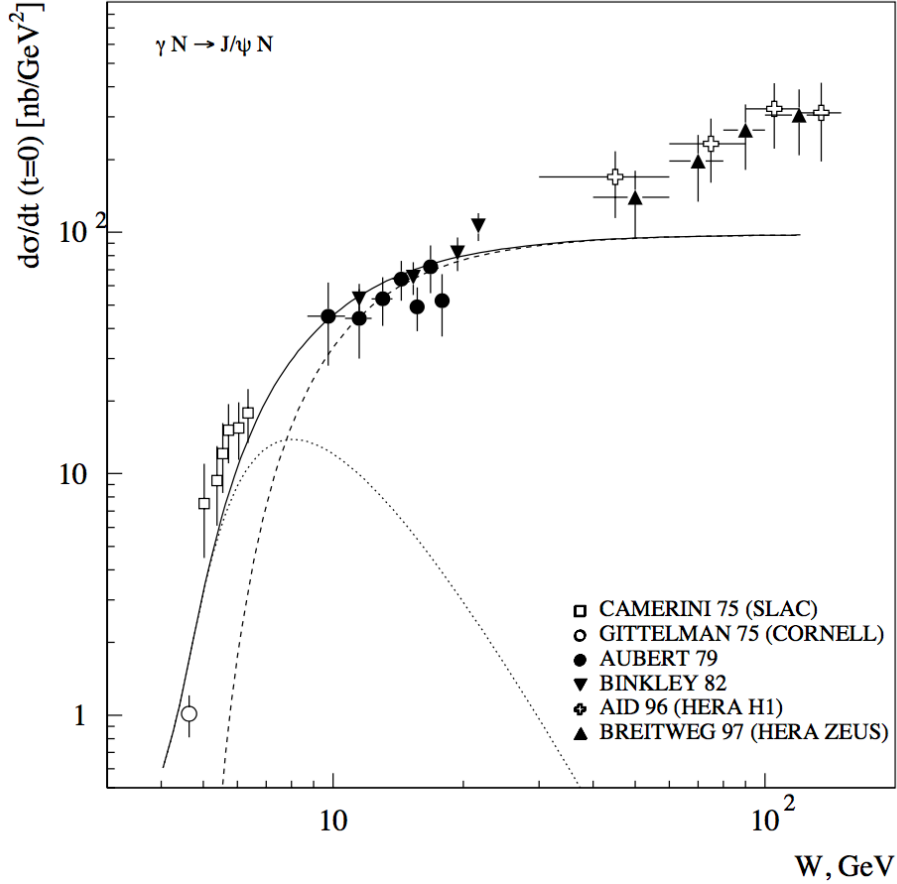


FIG. 3: Forward  $J/\psi$  photoproduction data compared to calculations of [13] with (solid line) and without (dashed line) the real part of the amplitude; the dotted line shows the real part alone.

- The newly discovered pentaquark  $P_c(4450)$  is considered as a bound state of charmonium  $\psi(2S)$  and the nucleon [17]. The binding potential is due to the charmonium-nucleon interaction that in the heavy quark approximation is proportional to the product of the charmonium chromoelectric polarizability and the nucleon energy-momentum distribution. Two almost degenerate states  $J^P = (1/2)^-$  and  $J^P = (3/2)^-$  are predicted at the position of the  $P_c(4450)$  pentaquark. The authors find that the nucleon- $\psi(2S)$  bound state has a naturally narrow width in the range of tens of MeV.
- One of the pentaquarks,  $P_c(4450)$  is interpreted [18] as a  $\chi_{c1}p$  baryo-charmonium composite resonance.
- The  $P_c$  states are interpreted as hadronic molecules [19–22]. These molecules consist of a charmed baryon and charmed meson which are weakly coupled with each other. Such

pentaquarks will decay predominantly to the charmed baryon and charmed meson.

- The pentaquarks are made of tightly correlated diquarks [23, 24] or colored baryon-like and meson-like constituents [25, 26].
- It has been also suggested that at least one of the peaks is not a resonance at all, but rather a kinematical singularity due to rescattering[24, 27–29] in the decay  $\Lambda_b \rightarrow J/\psi p K^-$ .

Clearly, resolving between the models and clarifying the nature of the discovered hidden-charm pentaquark peaks, and possibly searching for similar peaks with other quantum numbers, requires further experimental studies. These states were observed in the  $J/\psi + p$  decay mode. For this reason it is natural to expect that these states can be produced in the photoproduction process  $\gamma + p \rightarrow P_c \rightarrow J/\psi + p$  where they will appear as s-channel resonances at photon energy around 10 GeV [16, 30, 31]. Fig. 4 illustrates the S-channel pentaquark photoproduction process.

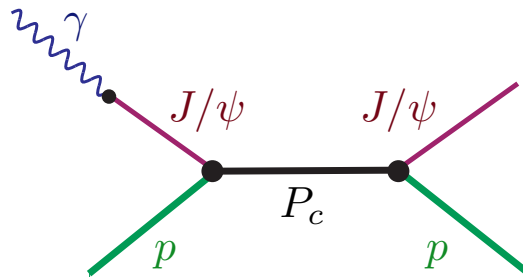


FIG. 4: Feynman diagram for the pentaquark photoproduction process.

Such experiments can be advantageous for detailed studies of the production and decay properties of the pentaquark resonances in comparison with the LHCb environment. The yield is determined by the branching fraction  $Br(P_c \rightarrow \gamma + p)$ , and it was shown [16] that this parameter can be expressed in terms of  $Br(P_c \rightarrow J/\psi + p)$  by a relation similar to vector dominance for the  $J/\psi$  photoproduction. Although such dominance cannot be justified as a general rule, in the situation at hand it can be applied due to arguments based on the heavy quark properties and special kinematics of the processes involved. As a result the peak cross section  $\sigma(\gamma + p \rightarrow P_c \rightarrow J/\psi + p)$  is proportional to  $Br^2(P_c \rightarrow J/\psi + p)$  and can reach tens of nanobarns or more, if  $Br(P_c \rightarrow J/\psi + p) \sim 1 - 10\%$ . Such relatively large cross section may allow fairly detailed studies of the pentaquarks and a search

for other similar states. In particular, it may be realistic to study the decays of the  $P_c$  states into  $J/\psi p\pi$  and  $J/\psi p\pi\pi$ . These types of decays should be prominent, if the  $P_c$  states are dominantly a baryo-charmonium, i.e. a hadro-quarkonium, type [32, 33] composite of  $J/\psi$  and excited nucleon states similar to the known resonances  $N(1440)$  and  $N(1520)$ . Such pattern of the decays of the  $P_c$  resonances would disfavor the molecular models [19–22], where one would expect the natural decay channels into a charmed hyperon and a meson, or from the  $\chi_{c1}p$  complex model [18], where the expected dominant decay is  $P_c(4450) \rightarrow \chi_{c1} + p$ . Naturally, any observation of the  $P_c$  peaks in the  $\gamma p$  cross section would strongly disfavor the interpretation [24, 27–29] in terms of ‘accidental’ singularities in the  $\Lambda_b$  decays.

### III. $J/\psi$ CROSS SECTION AND PRODUCTION RATES

Here we discuss the cross section formalism used to estimate rates for the proposed measurements. For real photoproduction, we use the same cross section model used to calculate rates for the experiment E-12-12-001 [2]. For electroproduction at very small  $Q^2$ , the Vector Dominance Model (VDM) [34] is used to relate photoproduction cross section to the electroproduction cross section.

#### A. Photoproduction cross section

The 2-gluon exchange formalism from [10] has been used to calculate the photoproduction cross section. This model for the  $J/\psi$  photoproduction on the nucleon, see Fig. 5, describes reasonably well the available data above  $E_\gamma = 11$  GeV as shown in Fig. 2. As presented in [10], the differential cross section can be written as

$$\frac{d\sigma_\gamma}{dt} = N_{2g}\nu \frac{(1-x)^2}{R^2 M^2} F_{2g}^2(t) (s - m_p^2)^2 \quad (3)$$

where  $F_{2g}(t)$  is the proton form factor that takes into account that the three target quarks recombine into the final proton after the emission of two gluons.  $M$  is the mass of the  $c\bar{c}$ ,  $R$  is the proton radius, taken as 1 fm,  $s$  is the center-of-mass energy squared and the  $x$  is the fraction of the proton momentum carried by the valence quark.  $N_{2g}$  is a scaling factor to saturate the measured cross sections as shown in Fig. 2. For the purposes of the rate estimate we used an exponential dependence for  $F_{2g}(t) \sim e^{bt}$ , with slope parameter  $b = 1.13$  GeV<sup>-2</sup> extracted from data. For the purposes of our rate estimate, the use of the 2-gluon model represents a conservative approach.

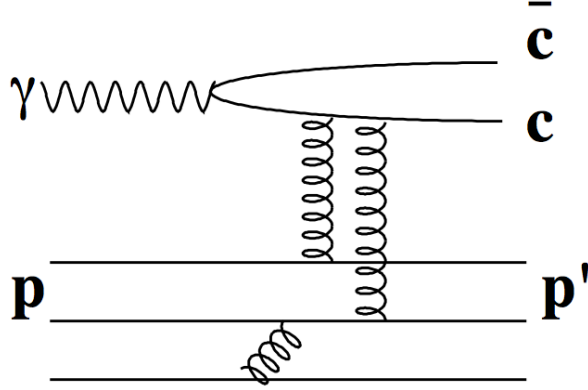


FIG. 5: Diagram for  $c\bar{c}$  photoproduction on the nucleon via 2-gluon exchange.

### B. Electroproduction cross section

The cross section for meson electroproduction can be decomposed in the sum of transversely ( $\sigma_T$ ), and longitudinally ( $\sigma_L$ ) polarized photon cross sections

$$\frac{d\sigma_{eN \rightarrow eM^0N}}{dQ^2 dW dt} = \Gamma_T \left( \frac{d\sigma_T}{dt} + \epsilon \frac{d\sigma_L}{dt} \right). \quad (4)$$

Here  $\Gamma_{\gamma^*}$  represents the flux of transverse virtual photons and is defined as:

$$\Gamma_T = \frac{\alpha}{4\pi} \cdot \frac{W^2 - m^2}{m^2 E^2} \cdot \frac{W}{Q^2} \cdot \frac{1}{1 - \epsilon}. \quad (5)$$

and the  $\epsilon$  is the ratio of longitudinal  $\Gamma_L$  to transverse  $\Gamma_T$  virtual photon fluxes

$$\epsilon = \left( 1 + 2 \frac{Q^2 + q_0^2}{4EE' - Q^2} \right)^{-1}. \quad (6)$$

Using vector meson dominance (VDM) one can relate  $\sigma_T$  and  $\sigma_L$  to the photoproduction cross section  $\sigma_\gamma$  [34]:

$$\sigma_T = \left( \frac{m_{J/\Psi}^2}{m_{J/\psi}^2 + Q^2} \right)^2 \cdot \sigma_\gamma, \quad (7)$$

and

$$\sigma_L = \left( \frac{m_{J/\Psi}^2}{m_{J/\psi}^2 + Q^2} \right)^2 \cdot \frac{Q^2}{m_{J/\psi}^2} \cdot (1 - x)^2 \cdot \xi(Q^2, \nu) \cdot \sigma_\gamma, \quad (8)$$

where  $m_{J/\psi}$  is the  $J/\psi$  meson mass. The  $\xi(Q^2, \nu)$  is a normalization parameter fitted to the experimental data. We used the value  $\xi(Q^2, \nu)=0.5$  in our calculations.  $x = Q^2/(2qp)$  where  $p$

is the four-momentum of the target nucleon. In the proposed measurement,  $Q^2 < 0.2 \text{ GeV}^2$ , and therefore we can assume  $\sigma_L \approx 0$  and  $\sigma_T \approx \sigma_\gamma$ , so that the electroproduction cross section for  $J/\psi$  can be expressed as:

$$\frac{d\sigma_{ep \rightarrow e' J/\psi p'}}{dQ^2 dW dt} = \Gamma_T \frac{d\sigma_\gamma}{dt} \quad (9)$$

### C. Pentaquark Photoproduction Cross Section

There have been already several publications that give estimates for photoproduction cross section of  $P_c(4380)$  and  $P_c(4450)$  [16, 30, 31]. The pentaquarks production proceeds as an  $s$ -channel resonance in the  $(J/\psi p)$  system. First, photon converts into the vector meson,  $J/\psi$ , which later is absorbed by the proton as shown in Fig.4 [35].

For a resonance  $P_c$  in the  $s$  channel, the photoproduction cross section of the reaction  $\sigma(\gamma + p \rightarrow P_c \rightarrow J/\psi + p)$  is given by the standard Breit-Wigner expression (see e.g. in Ref. [36], Sec. 48.1.)

$$\sigma(W) = \frac{2J+1}{4} \frac{4\pi}{k^2} \frac{\Gamma^2/4}{(W - M_c)^2 + \Gamma^2/4} Br(P_c \rightarrow \gamma + p) Br(P_c \rightarrow J/\psi + p) , \quad (10)$$

where  $J$  is the spin of the  $P_c$  resonance,  $W = \sqrt{s}$  is the c.m. energy,  $M_c$  is the resonance mass,  $\Gamma$  is the total width and  $k$  is the center of mass (c.m.) momentum of the colliding particles. At the maximum of either of the  $P_c$  resonances this expression gives numerically (at  $k \approx 2.1 \text{ GeV}$ )

$$\sigma_{max}(\gamma + p \rightarrow P_c \rightarrow J/\psi + p) \approx \frac{2J+1}{4} Br(P_c \rightarrow \gamma + p) Br(P_c \rightarrow J/\psi + p) 1.1 \times 10^{-27} \text{ cm}^2 . \quad (11)$$

The actual value of the cross section in Eq.(11), naturally, depends on the product of the branching fractions, neither of which is presently known. However, the branching fraction  $Br(P_c \rightarrow \gamma + p)$  can be estimated in terms of  $Br(P_c \rightarrow J/\psi + p)$  in a way that does not directly rely on a specific model of the internal dynamics of the pentaquarks, but which is somewhat sensitive to the structure of the amplitude of the decay  $P_c \rightarrow J/\psi + p$ .

It was shown in [16] that the bounds for the formation cross section at the resonance maximum assuming the quantum numbers  $J^P = (3/2)^-$  and  $(5/2)^+$  respectively for  $P_c(4380)$  and  $P_c(4450)$  are:

$$\begin{aligned} 1.5 \times 10^{-30} \text{ cm}^2 &< \frac{\sigma_{max}[\gamma + p \rightarrow P_c(4380) \rightarrow J/\psi + p]}{Br^2[P_c(4380) \rightarrow J/\psi + p]} < 47 \times 10^{-30} \text{ cm}^2 , \\ 1.2 \times 10^{-29} \text{ cm}^2 &< \frac{\sigma_{max}[\gamma + p \rightarrow P_c(4450) \rightarrow J/\psi + p]}{Br^2[P_c(4450) \rightarrow J/\psi + p]} < 36 \times 10^{-29} \text{ cm}^2 , \end{aligned} \quad (12)$$

where the lower bound corresponds to the presence of only the lower allowed partial wave, while the upper bound is found in the opposite situation where only the higher orbital wave is present. Currently neither branching fraction  $Br(P_c \rightarrow J/\psi + p)$  is known, nor the spin-parity quantum numbers for the observed pentaquarks are determined with certainty. Thus, it is not possible to estimate more definitely the value of the discussed formation cross section in a model independent way.

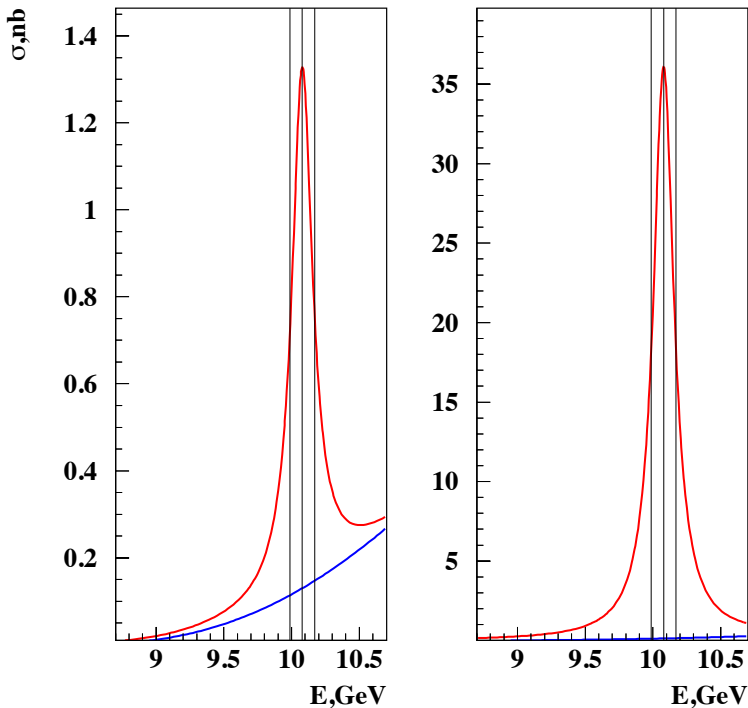


FIG. 6: The  $P_c(4450)$  resonance formation cross section in the reaction  $\gamma p \rightarrow P_c \rightarrow J/\psi p$  as a function of the photon energy in the region of the CLAS12 acceptance. Two panels represent the theoretical uncertainty due to the unknown composition of the partial waves (see text for details). The vertical lines represent the resonant energy  $E_0 = 10.1$  GeV and the boundaries of the region  $M_c \pm \Gamma/2$  (see Eq. 11) in the laboratory system. The two curves show the elastic background [10] and Breit-Wigner distribution. The calculations were done assuming  $Br(P_c \rightarrow J/\psi p) = 1\%$ . The cross section is proportional to  $Br^2(P_c \rightarrow J/\psi p)$ .

The  $J/\psi$  photoproduction cross section using 2-gluon exchange model described above was used to estimate the elastic background under the pentaquark peaks, shown as a red line in Fig. 2. The

model-dependent extrapolation to the region of interest gives a cross section of  $\sim 0.1$  nb.

Fig. 6 illustrates the  $P_c(4450)$  pentaquark formation cross section as a function of the photon beam energy in the CLAS12 acceptance region for two cases. The left panel corresponds to the presence of only the lower allowed partial wave. The right panel shows the same cross section for the upper bound where only the higher orbital wave is present (see Eq. 12). The vertical lines represent the resonant energy  $E_0 = 10.1$  GeV and the boundaries of the region  $M_c \pm \Gamma/2$  (see Eq. 11) in the laboratory system that contains 50% of the total production cross section. The calculations were done with  $Br(P_c \rightarrow J/\psi p) = 1\%$ . It is worth to mention that a rigorous analysis of the existing  $J/\psi$  elastic photoproduction data [37] demonstrated that, for  $P_c(4450)$ , a branching fraction  $Br(P_c \rightarrow J/\psi p)$  up to  $8 \div 17\%$  cannot be excluded within 90% CL. The model for pentaquark production in that analysis is almost equivalent to the one employed in this work, and considered different values for the  $E_\gamma$  resolution.

#### IV. PROPOSED EXPERIMENT

In this proposal we aim to study  $J/\psi$  production on hydrogen using the tagged and untagged photoproduction techniques. Both techniques will be used by the already approved CLAS12 experiments, E12-11-005 and E12.12-001, to study meson spectroscopy, time-like Compton scattering, and  $J/\psi$  production. The reaction:

$$ep \rightarrow e'p'J/\psi \quad (13)$$

will be measured by detecting different final states identifying the  $J/\psi$  meson and the charmed pentaquarks using the missing mass or the invariant mass analysis. The different methods have different mass resolution, different  $J/\psi$  detection rates, and are sensitive to different backgrounds. In the tagged photoproduction case scattered electron will be detected in the CLAS12 Forward Tagger (FT) while recoil proton and leptons from the  $J/\psi$  decay (electron or  $\mu$ ) will be detected in the CLAS12 Forward Detector (FD). In this case the  $J/\psi$  will be identified using the missing mass technique by measuring the scattered electron and recoil proton, while the pentaquarks will be identified in the  $W$  distribution calculated from the scattered electron 3-momentum. In the untagged electroproduction case the recoil proton and both decay leptons will be detected in FD. The  $J/\psi$  will be reconstructed in the lepton pair invariant mass, pentaquarks will be identified in the invariant mass of  $J/\psi -$  proton system.

### A. Photon flux

The photon flux for electroproduction at  $Q^2 \sim 0$  has been calculated for the two cases. In the untagged photoproduction case, when scattered electron is not detected the total flux of photons is the sum of the virtual photon flux  $\Gamma_{\gamma^*}$  given in Eq.(5), and the flux of real photons produced from electrons bremsstrahlung in the target. The virtual photon flux was estimated as a function of  $W$  by integrating  $\Gamma_{\gamma^*}$  from kinematically allowed  $Q_{min}^2$  to some  $Q_{max}^2$  beyond which the change in the flux is not significant.

$$\Gamma_W = \int_{Q_{min}^2}^{Q_{max}^2} \Gamma_{\gamma^*} dQ^2 \quad (14)$$

For electron bremsstrahlung, the standard formula has been used [36]:

$$n(E_\gamma) = \int_{E_\gamma^{min}}^{E_\gamma^{max}} \frac{l}{2 \cdot X_0} \frac{1}{E_\gamma} \cdot \left( \frac{4}{3} - \frac{4 E_\gamma}{3 E_b} + \frac{E_\gamma^2}{E_b^2} \right) dE \quad (15)$$

where  $E_b$  is the beam energy,  $l$  is the thickness of the target and the  $X_0$  is the radiation length of the target material. The total equivalent photon beam luminosity (sum of virtual and real photon fluxes) for an electron luminosity  $L = 10^{35} \text{ cm}^{-2} \text{ sec}^{-1}$  as a function of the total center-mass energy in 0.02 GeV energy bins is shown in Figure 7 by a solid line.

To obtain the flux for tagged photoproduction case, the angular acceptance of the Forward Tagger, where scattered electrons will be detected, has to be considered, i.e.  $2.5^\circ < \theta' < 4.5^\circ$ . This gives:

$$\begin{aligned} d\Gamma(E') &= \frac{\alpha}{4\pi} \frac{\nu}{E_0^2} \left[ \frac{(2E_0 - \nu)^2}{\nu^2} + 1 \right] \log \left( \frac{1 - \cos \theta_{max}}{1 - \cos \theta_{min}} \right) dE' \\ &\simeq 1.1 \cdot \frac{\alpha}{4\pi} \frac{\nu}{E_0^2} \left[ \frac{(2E_0 - \nu)^2}{\nu^2} + 1 \right] dE' \end{aligned} \quad (16)$$

or:

$$d\Gamma(W) \simeq 1.1 \cdot \frac{\alpha}{4\pi} \frac{\nu}{E_0^2} \left[ \frac{(2E_0 - \nu)^2}{\nu^2} + 1 \right] \frac{W}{M_p} dW \quad (17)$$

The luminosity of tagged photons is shown in Figure 7 as a dashed-dotted line. In the energy range from  $J/\psi$  production threshold to 11 GeV, the untagged photon flux is an order of magnitude larger than tagged photon flux.

### B. Untagged photoproduction

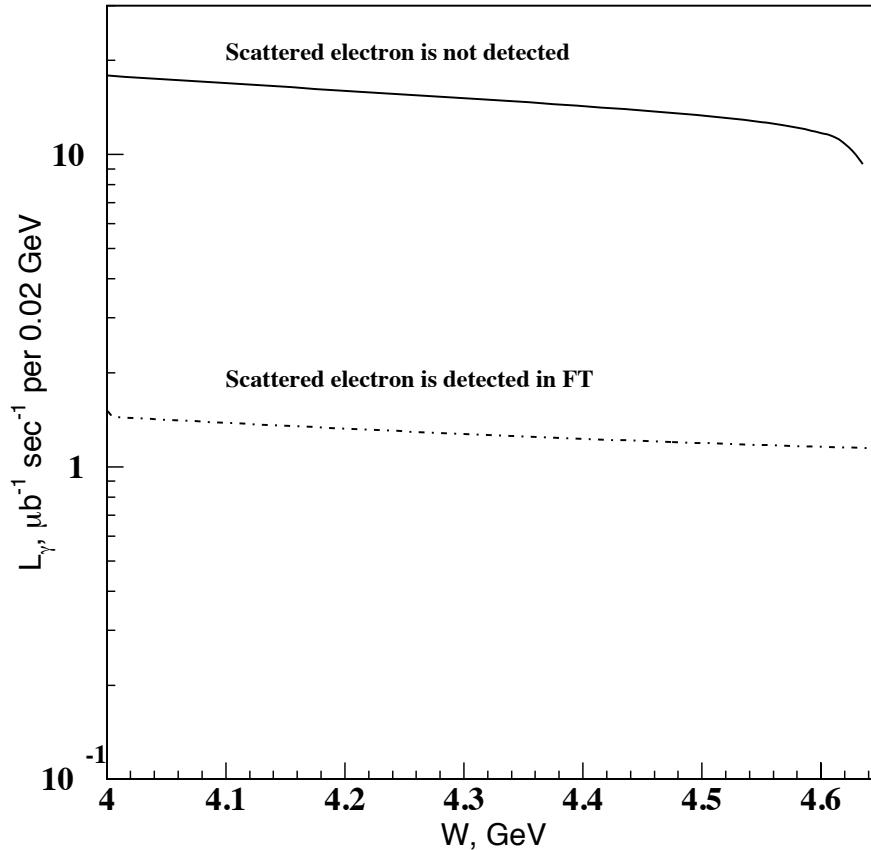


FIG. 7: Comparison of effective luminosities for untagged and tagged electroproduction cases.

The experiment E12-12-001 [2] will study Time-like Compton Scattering (TCS) and the photoproduction of  $J/\psi$  near threshold in the reaction

$$ep \rightarrow p'e^+e^-(e'). \quad (18)$$

where ( $e'$ ) denotes undetected scattered electron,  $p'$  is the recoil proton,  $e^+$  and  $e^-$  are the  $J/\psi$  decay products. All three particles will be detected in CLAS12 FD. The scattered electron kinematics will be reconstructed from the missing momentum analysis. Requiring the missing momentum to be in the direction of the beam,  $\theta_x \sim 0$ , and the missing mass to be  $m_x \simeq 0$ , one effectively selects events from the quasi-real photoproduction of electron pairs off hydrogen. This technique has been successfully used for analysis of the CLAS 6 GeV electroproduction data and has been proven to be excellent way to study photoproduction reactions when all particles in the final state are detected (see [38, 39]).

The main goal of the  $J/\psi$  studies proposed in E12-12-001 is to measure the total cross section near the threshold and study the  $t$ -dependence that can shed light on nucleon gluonic form-factors. The LHCb pentaquarks, discovered in the invariant mass of  $(J/\psi p)$ , fall exactly in the middle of the energy range of this experiment and can be searched and studied with the same experimental setting. In addition, we propose to perform  $J/\psi$  and pentaquark studies using the reaction:

$$ep \rightarrow p' \mu^+ \mu^- (e'). \quad (19)$$

where  $J/\psi$  decays to muon pairs. Adding this decay mode will double the statistics. The kinematics of muons and electrons from  $J/\psi$  decay are very similar so the CLAS12 efficiency will be the same for muon pair detection. Of course the major concern for this final state is the  $\pi^+\pi^-$  background (when pion is misidentified as a muon).

In the reaction reported in Eq.19 the scattered electron will be identified using the missing momentum analysis. This selection will insure that the background from three or more pion final states will be negligible. The total cross section for the reaction  $\gamma p \rightarrow p' \pi^+ \pi^-$  at energies  $E_\gamma \simeq 10$  GeV is about  $15 \mu\text{b}$  [40]. In Fig. 8, distribution of events as a function of two-pion invariant mass is shown for this reaction at  $E_\gamma = 20$  GeV from [41]. As one can see, among all possible contributions to exclusive two pion final state, the dominant contribution is from  $\rho^\circ$  and  $\rho''$ . The fraction of pion pairs with the invariant mass  $> 3$  GeV is less than  $\sim 2 \times 10^{-4}$ , so the effective cross section for pion pair photoproduction with the invariant mass in the region of  $J/\psi$  is expected to be  $< 5$  nb.

While CLAS12 does not have a dedicated muon detector, the CLAS12 forward calorimeter (ECAL, combined PCAL and EC together) where muons from  $J/\psi$  decay will be detected, have some rejection power to pions. Studies using GEANT-4 model of the CLAS12, GEMC, and the event reconstruction framework CoatJava show that a significant number of charged pions will produce hadronic shower in the calorimeter releasing in ECAL more energy than what one expect for a MIP. In Fig. 9, the fraction of charged pions surviving the selection cuts on total energy in ECAL,  $< 200$  MeV, and in the EC-outer,  $< 100$  MeV, is shown as a function of pion momentum. The fraction is almost independent of pion momentum and is  $\sim 40\%$ . The same cuts retain 97% of muons. This cuts alone can reach at least  $\times 6$  suppression of charged pion pairs relative to muon pairs. More selection cuts can be developed by looking also cluster (pixel) size. This factor brings down the rate of pion pairs in the region of the invariant mass  $> 3$  GeV to the same order as  $J/\psi$  rate.

Some MC studies for  $J/\psi$  photoproduction near the threshold, covering the region of the charmed pentaquarks are reported below. Simulations were performed with a Fast-MC and a full

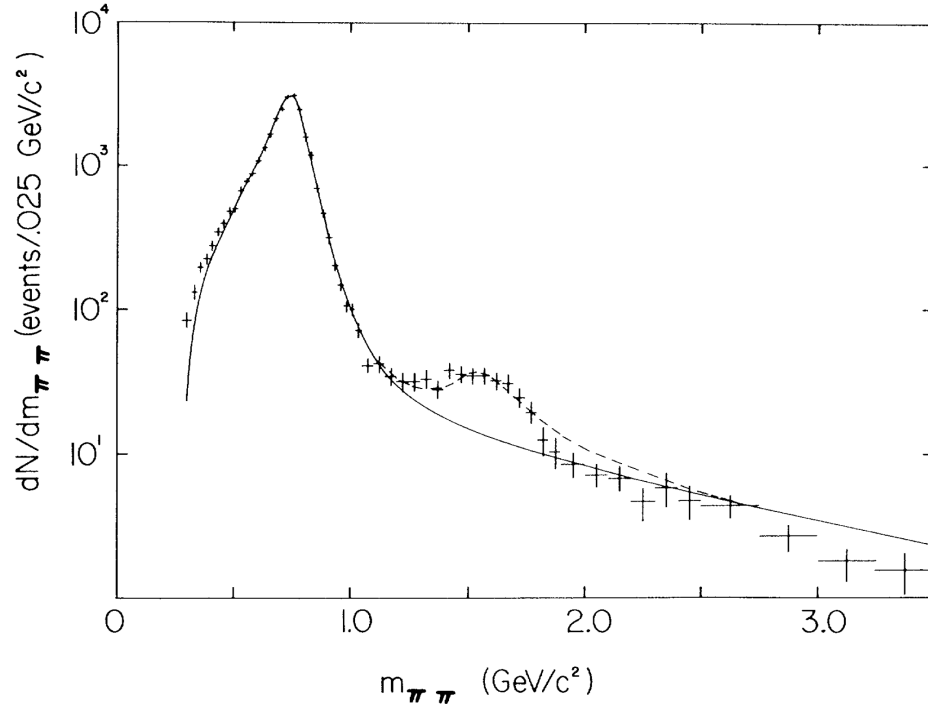


FIG. 8: Invariant mass distribution of  $\pi^+\pi^-$  in the reaction  $\gamma p \rightarrow p'\pi^+\pi^-$  at  $E_\gamma = 20$  GeV.

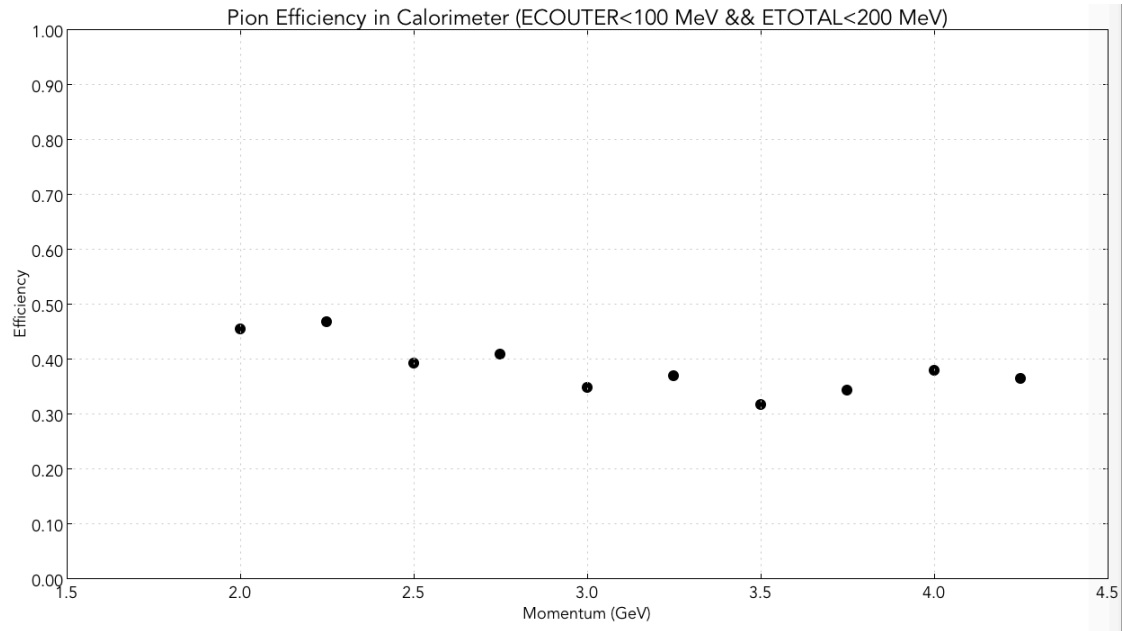


FIG. 9: Efficiency of charged pion detection in ECAL after requiring the total energy deposition to be  $< 200$  MeV and the energy deposition in the outer EC  $< 100$  MeV.

GEANT4 model of the CLAS12 detector. We checked the detection efficiency and the mass resolutions for different final states for one setting of the torus magnet (full field) using the up-to-date GEANT-4 based CLAS12 simulation tool, GEMC, and the event reconstruction code, CoatJava. The results of full simulation and reconstruction agreed very well with Fast MC results. Particle identification was not the part of these studies, besides pion/muon separation studies reported above. The CLAS12 Fast MC does not have PID scheme, and the particle identification is not fully implemented in CoatJava. However, we do not see any challenges in PID for the proposed measurements. The CLAS12 electron identification scheme, based on the high threshold Cerenkov counter (HTCC) and the electromagnetic calorimeter, are sufficient for identification of  $e^+e^-$  pairs from  $J/\psi$  decay. The recoil protons are in 1 GeV/c to 3 GeV/c momentum range and the time resolution of the CLAS12 forward time-of-flight system (FTOF) (100 ps) is sufficient to separate protons from kaons and pions in this momentum range. Similarly, forward tagger is well suited to detect electrons from few hundred MeV to few GeV range.

### 1. Kinematics

With a beam energy of 11 GeV, all three final state particles, a recoil proton, and the decay leptons from  $J/\psi$  photoproduction will be detected in CLAS12 FD. In Fig. 10, the scattering angle ( $\theta$ ) in the lab reference frame is plotted against particle momentum ( $p$ ) for protons on the left, and for electrons and positrons on the right in the kinematics of the untagged photoproduction (quasi-real photoproduction of  $J/\psi$  in photon energy range from threshold to 11 GeV). Kinematics of the reaction is simulated with the expected  $s$ - and  $t$ -dependences of the cross section (see below). As can be seen all three final state particles are energetic and are produced in forward direction. There are some electrons at large angles,  $\theta > 35^\circ$ , however since the CLAS12 Central Detector (CD) is not suited for electron detection and identification we will consider CLAS12 FD acceptance only.

In Fig. 11 the efficiency for detecting all three final state particles CLAS12 FD is shown as a function of photon beam energy. The efficiency is about 10% for the maximum torus field setting and arises slowly with lowering the field. In Fig. 12, the invariant mass distribution for the detected ( $pe^+e^-$ ) system is presented. The charmed pentaquarks are in the center of the mass acceptance in the kinematics of the untagged photoproduction.

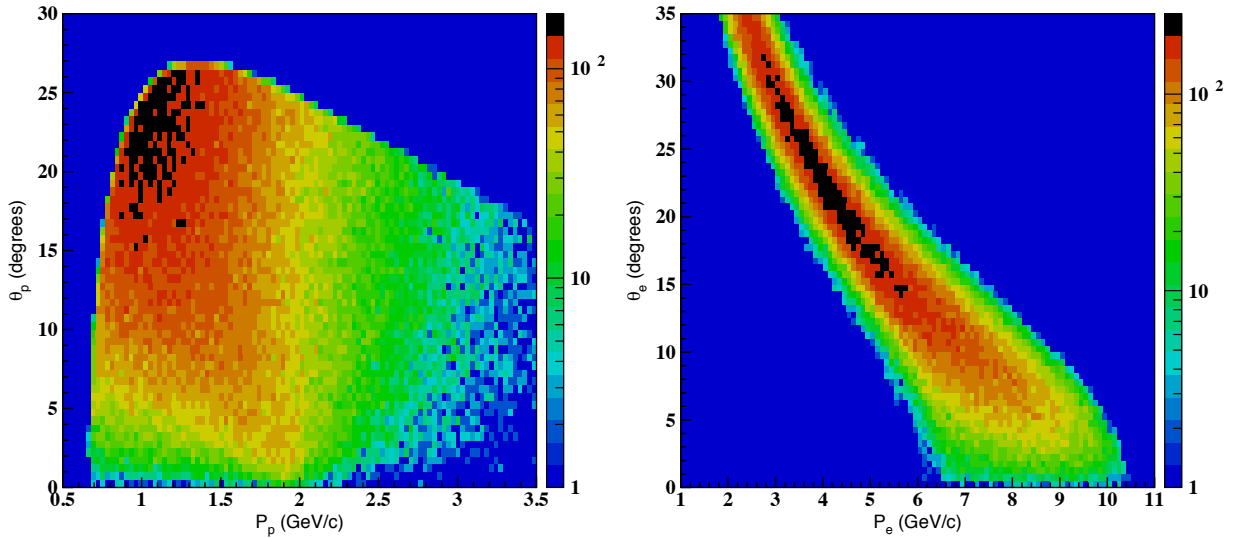


FIG. 10: Scattering angle vs. momentum for protons (left) and electrons ( $e^-$ ,  $e^+$ ) (right) in the reaction  $ep \rightarrow J/\psi p(e')$  for quasi-real photon energies from the threshold to 11 GeV.

## 2. Mass resolutions

A reasonably good mass resolution is required to search for pentaquark states, especially for the narrow  $P_c(4450)$  state. In the analysis the  $J/\psi$  will be identified in the invariant mass distribution of  $(e^+e^-)$ . The identification of the pentaquarks will be done by searching for a peak in the  $(J/\psi p)$  invariant mass. Studies have been conducted to explore the effect of the torus field setting on these invariant mass resolutions using the CLAS12 FastMC. In Fig. 13, results of these studies are shown. The invariant mass resolutions have been checked with GEANT-4 simulation (GEMC, model of the CLAS12) and the CLAS12 event reconstruction code, CoatJava, for full field setting of the torus magnet. In Fig. 14, Considering the expected background under the  $J/\psi$  peak and the narrow width of  $P_c(4450)$ ,  $\sim 40$  MeV, we concluded that torus field setting above 60% of the max will be acceptable for these measurements. There was no effect observed on the mass resolution from the solenoid field value, so we will accept any setting that allows running at the proposed luminosity or higher.

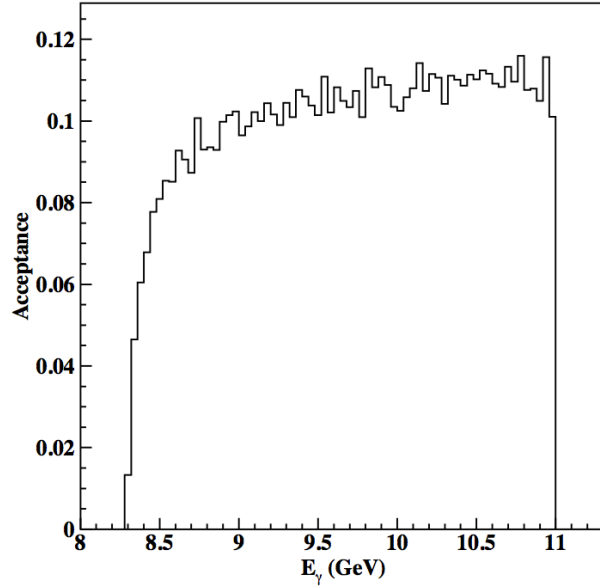


FIG. 11: Acceptance simulated using CLAS12 Fast-MC for  $(pe^-e^+)$  in the reaction  $ep \rightarrow J/\psi p(e') \rightarrow e^+e^-p(e')$  for quasi-real photon energies from the threshold to 11 GeV.

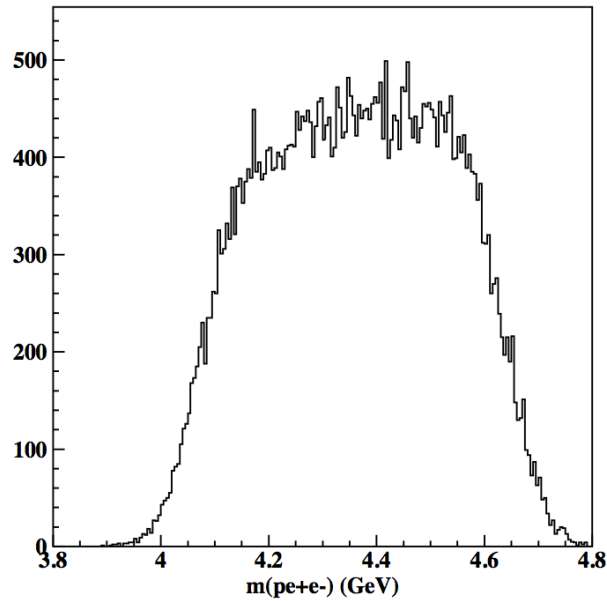


FIG. 12: Mass distribution of  $(pe^-e^+)$  in the reaction  $ep \rightarrow J/\psi p(e') \rightarrow e^+e^-p(e')$  for quasi-real photon energies from the threshold to 11 GeV. The smeared in Fast-MC values of momenta and angles are used to calculate the invariant mass.

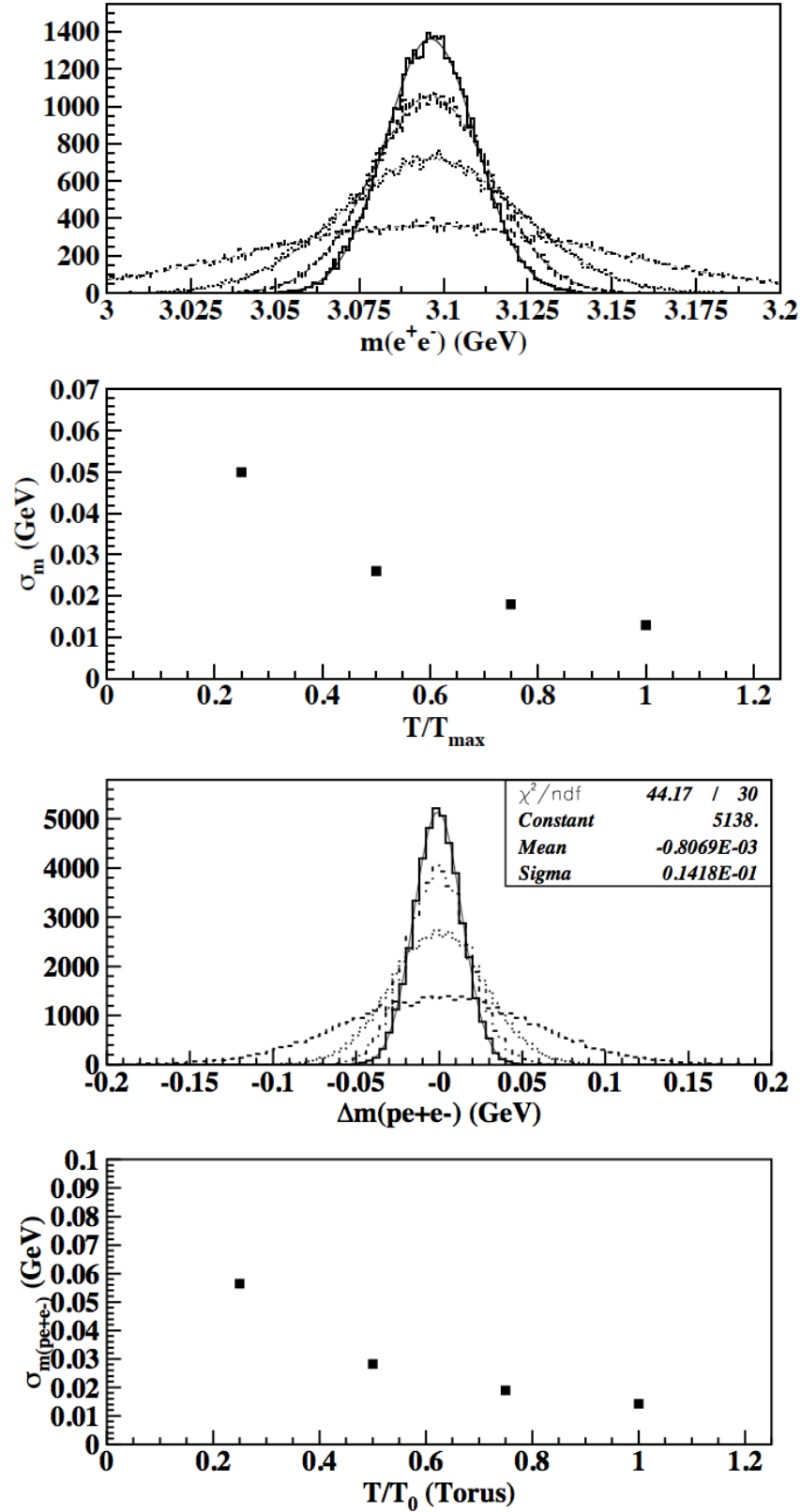


FIG. 13: The  $e^+e^-$  invariant mass resolution at  $J/\psi$  mass as function of CLAS12 torus field settings. The  $pe^+e^-$  invariant mass resolution as a function of CLAS12 torus field settings. The  $(e^+e^-)$  are from  $J/\psi$  decay. The CLAS12 Fast-MC is used for these estimates.

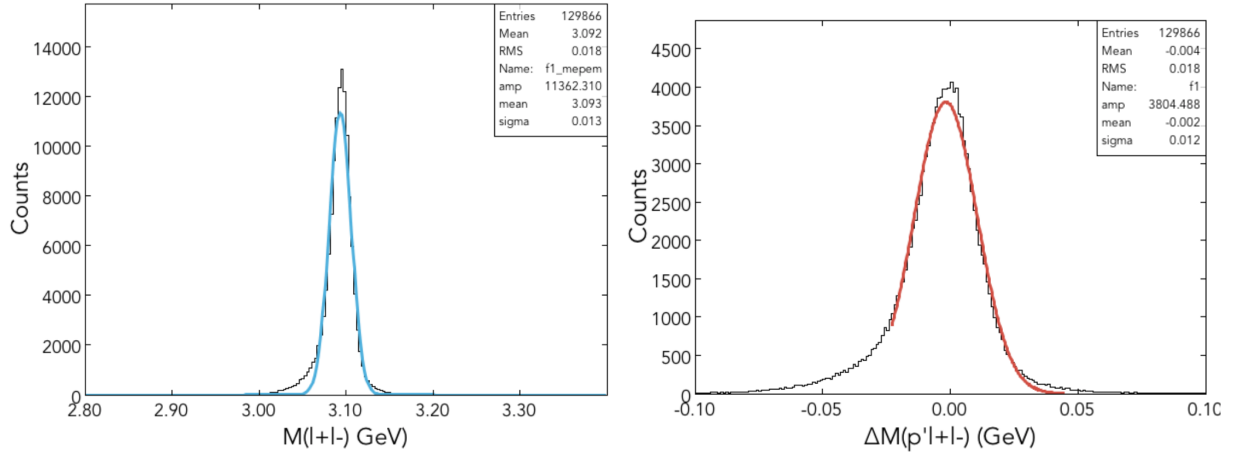


FIG. 14: The  $e^+e^-$  and  $pe^+e^-$  invariant mass distributions from GEMC/CoatJava simulations and reconstruction for the full field setting of the torus magnet.

### 3. Estimate of the pentaquark yield

The expected rates for  $J/\psi$  production, and statistical accuracy for measuring  $t$ - and energy dependences have been detailed in E12-12-001 proposal [2]. Here we present the expected rates for pentaquarks ( $E_\gamma \simeq 10$  GeV) based on the cross section formalism presented in Section III.

In order to calculate the expected rates, one should also take into account a  $BR(J/\psi \rightarrow e^+e^-) \simeq 0.06$  and the detector efficiency (acceptance) of  $\epsilon \simeq 0.1$  in the pentaquark mass range. With the assumption of the 2-gluon exchange and no pentaquarks, the cross section at 10 GeV is  $\sim 0.08$  nb and the expected total number of  $J/\psi$  mesons in the  $\Delta W = 20$  MeV ( $pe^+e^-$ ) mass bin is about 1/day with the nominal CLAS12 luminosity. Note that the studies proposed in E12-12-001 will be done in much larger bins of  $W$ .

The total number of the events in CLAS12 for the reaction  $\gamma p \rightarrow P_c \rightarrow J/\psi p$ ,  $J/\psi \rightarrow e^+e^-$  was estimated as:

$$N(P_c) = \int \sigma(W) \frac{dL_\gamma}{dW} \epsilon dW \cdot Br(J/\psi \rightarrow e^+e^-) = 0.5 \int \sigma(W) dW \text{ events/nb/MeV/day} \quad (20)$$

where  $\frac{dL_\gamma}{dW} = 10^{30}$  events/cm<sup>2</sup>/MeV/s =  $10^{-3}$  events/nb/MeV/s is the CLAS12 photon luminosity per  $\Delta W = 1$  MeV bin at the nominal electron-proton luminosity  $L_{ep} = 10^{35}$  cm<sup>-2</sup> sec<sup>-1</sup>. The pentaquark yield for one day at this luminosity is presented in Table I for two states and two values of the predicted cross sections shown in Fig. 6, assuming  $Br(P_c \rightarrow J/\psi p) = 1\%$ .

These rates are only for one decay channel,  $J/\psi \rightarrow e^+e^-$ . The same reaction will be studied in the same way in  $J/\psi \rightarrow \mu^+\mu^-$  decay mode. This decay mode was not considered in E12-12-001

TABLE I: Estimated number of detected pentaquarks per day.

	Number of events per day, minimum-maximum
$P_c(4380)$	24 - 750
$P_c(4450)$	35 - 1100

due to the trigger requirement, to be compatible with the standard CLAS12 electron trigger.

### C. Tagged electroproduction

Tagged  $J/\psi$  electroproduction at low  $Q^2$  (quasi-real photoproduction) will be measured as part of the experiment E12-11-005 (MesonEx) through the reaction

$$e p \rightarrow e' p' J/\psi$$

with the final state electron scattered at low angle and measured in the Forward Tagger detector. The final state proton and the  $J/\psi$  decay products, instead, will be measured in the CLAS12 FD. Both the decay channels  $J/\psi \rightarrow e^+e^-$  and  $J/\psi \rightarrow \mu^+\mu^-$  will be investigated. For the latter, muon-pion discrimination in the CLAS12 FD is crucial: as discussed in the previous section, preliminary studies show that a rejection factor up to x6 can be reached, thus bringing down the rate of pion pairs in the  $J/\psi$  region to the same order as the  $J/\psi \rightarrow \mu^+\mu^-$  channel. The estimates reported in the following are performed conservatively just considering the cleaner  $J/\psi \rightarrow e^+e^-$  channel.

Compared to the untagged electroproduction case previously discussed, the tagged experiment has an expected event rate of about 1/10, due to the lower equivalent photon flux (see Figure 7). This is a direct consequence of the lower cut-off on the  $\theta'$  scattering angle imposed by the FT acceptance. However, in this case the invariant mass  $W$  of the  $J/\psi p$  system can be measured as the missing mass of the final state electron, that depends only on the measured energy in the Forward Tagger. This resolution is independent of the torus field setting and more than a factor 2 better than in the untagged photoproduction case. Explicitly,

$$W^2 = M_p^2 + 2E_0M_p - 2E'M_p \quad , \quad (21)$$

Therefore, close to the mass region where resonances are expected, one has:

$$\sigma_W = \sigma_{E'} \cdot \frac{M_p}{W} \simeq 0.21 \cdot \sigma_{E'} \simeq 5.2 \text{ MeV} \quad , \quad (22)$$

being  $\sigma_{E'} \simeq 25 \text{ MeV}$  the expected energy resolution for the final state electron measured in FT [42] for  $E' \simeq 1 \text{ GeV}$ . This value is significantly lower than the resonance width reported by LHCb for the narrower  $P_c$  state,  $\Gamma = 39 \text{ MeV}$ , demonstrating that MesonEx is capable of properly determining the resonance line-shape.

In the following, we discuss the kinematic properties of the events measured in the tagged measurement, the possible measurement strategies, and the expected pentaquark yield.

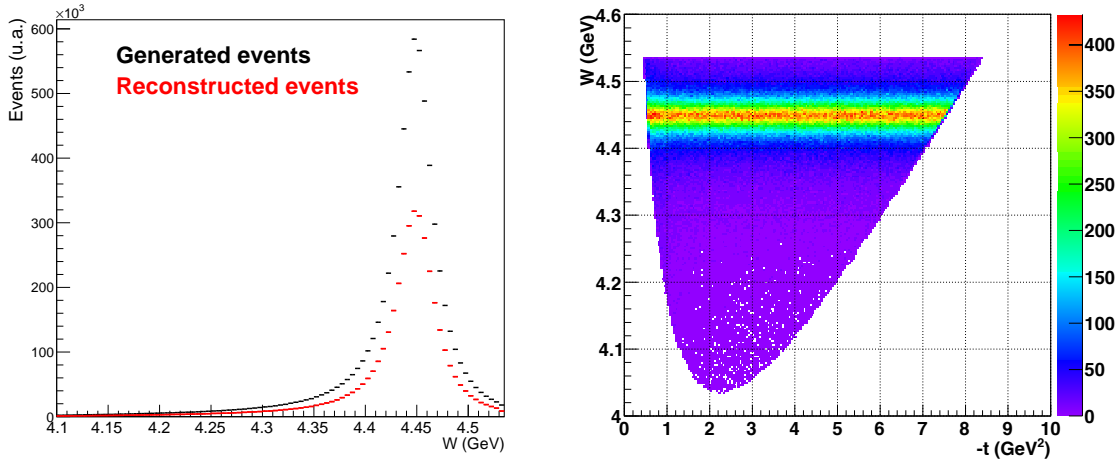


FIG. 15: Left:  $pJ/\psi$  invariant mass distribution for generated and reconstructed events. Right:  $pJ/\psi$  invariant mass vs momentum transfer on the proton distribution.

### 1. Kinematics

The distribution of the  $p'J/\psi$  invariant mass ( $W$ ) is reported in Fig. 15, together with the correlation between  $W$  and the momentum transferred to the proton,  $-t$ . The  $W$  distribution is shown for both generated and reconstructed events - assuming a two-charged particles topology, as discussed below. The momentum vs. angle distribution for proton and leptons, in the laboratory frame, is plotted in Fig. 16. The proton is always emitted at low angles,  $\theta_P < 25^\circ$ , due to the lower mass with respect to the  $J/\psi$  meson. The  $e^+$  and the  $e^-$ , instead, are typically emitted at larger angles, with a significant fraction of events with one or both leptons out of the CLAS12-FD acceptance.

### 2. Detector response

The reaction that we consider has 4 particles in the final state: a low-angle scattered electron, measured with the Forward Tagger, and a proton and an electron-positron pair from  $J/\psi$  decay, measured with the CLAS12 detector. Since the CLAS12-Central Detector (CD) is not suited for electron detection and identification, we consider only the detection of final state leptons in the CLAS12-Forward Detector (FD). Different measurement strategies are possible:

- Measure *all* the final state particles, reconstructing the  $J/\psi$  via the invariant mass of the electron-positron pair.

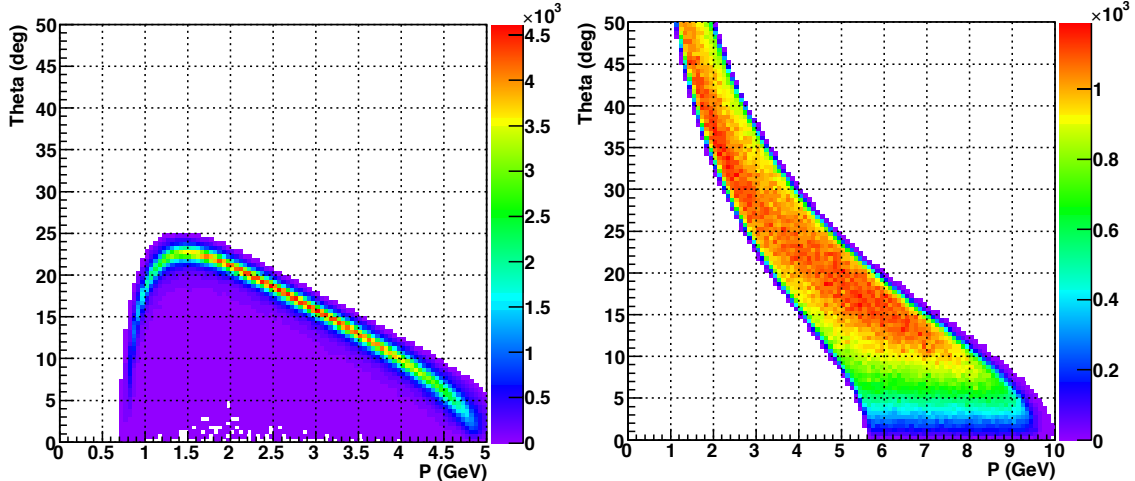


FIG. 16: Momentum-vs-angle distribution for the final state proton (left) and for the leptons (right), in the laboratory frame.

- Measure the scattered electron in the Forward Tagger and the electron-positron pair in the CLAS12-FD, reconstructing the  $J/\psi$  via the invariant mass of the  $e^+e^-$  system and identifying the proton using the missing mass of all detected particles.
- Measure the scattered electron in the Forward Tagger, and the proton and one of the leptons in the CLAS12-FD, reconstructing the  $J/\psi$  via the proton missing mass.

While the first option would permit a better background discrimination, given the larger control on kinematics variable that the full measure of the final state allows, the second and the third - complementary to each other - result in a slightly larger experimental acceptance.

The CLAS12 and Forward Tagger response was simulated using the Fast MonteCarlo (FASTMC) code, that effectively accounts for the detector geometrical acceptance and resolution. Each final state particle, i.e. the recoil proton, the scattered electron, and the two leptons, is projected individually on the detector. If it is within the nominal detector acceptance region, the four-momentum is smeared according to the expected resolution, otherwise it is discarded. We made the following conservative assumptions:

- The CLAS12-CD acceptance for leptons is zero. As discussed, this reflects the fact that this detector is not designed for  $e^-/e^+$  detection and identification.
- We considered only events with both the electron and the positron from  $J/\psi$  decay detected in the CLAS12-FD, i.e. we neglected the possibility that they are measured in the Forward Tagger.

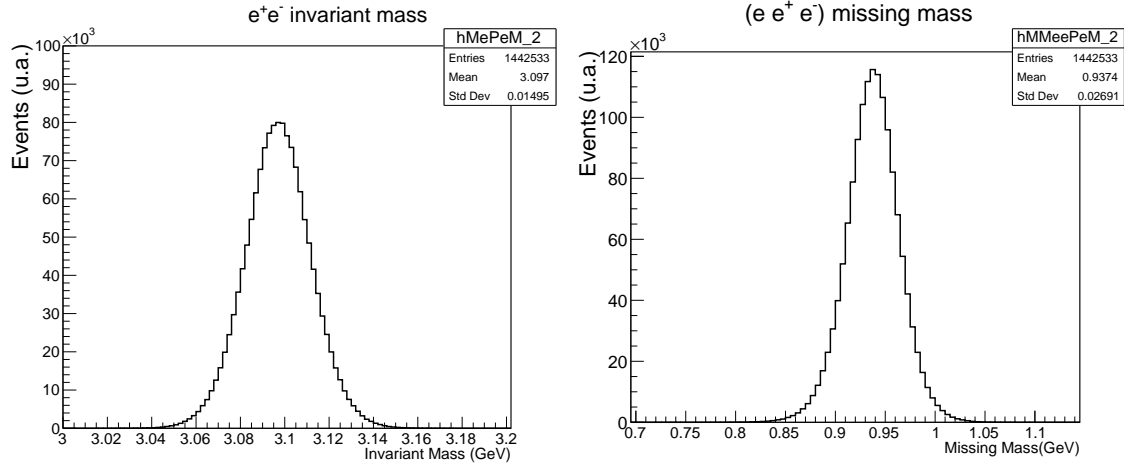


FIG. 17:  $e^+e^-$  final state. Left: reconstructed  $J/\psi$  mass. Right: missing mass of the  $e'e^+e^-$  system. Plots refer to the maximum value of the CLAS12 toroidal field, configured to have positive particles outbending.

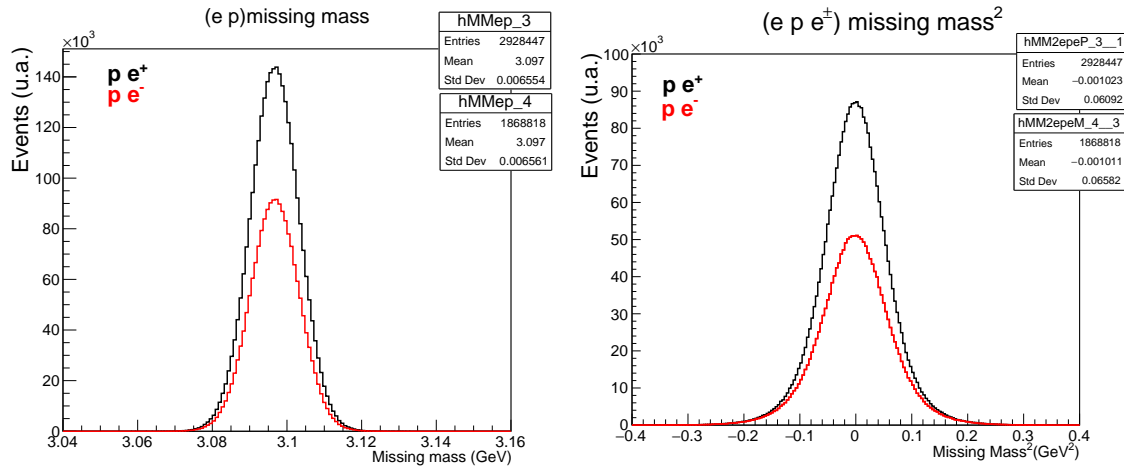


FIG. 18:  $pe^-$  and  $pe^+$  final state. Normalization of histograms reflects different CLAS12 acceptance for the two final states. Left: reconstructed  $J/\psi$  mass. Right: missing mass squared on the electron-proton-lepton system. Plots refer to the maximum value of the CLAS12 toroidal field, configured to have positive particles outbending.

Figure 17 shows relevant quantities for the reconstruction of the final state when the electron and the positron are measured: the invariant mass of the two leptons - showing the  $J/\psi$  peak, and the  $e^-e^+$  missing mass, where the proton is reconstructed. The two resolutions, in case of maximum value of the CLAS12 toroidal field, configured to have positive particles outbending, are respectively 15 MeV and 27 MeV. Figure 18, instead, shows kinematic quantities that are relevant for the  $pe^+$  and  $pe^-$  measurements, the proton missing mass distribution and the proton-lepton missing mass distribution. The two final states are characterized by the same experimental resolution for these observables, of about 6 MeV and  $0.06 \text{ GeV}^2$ , respectively.

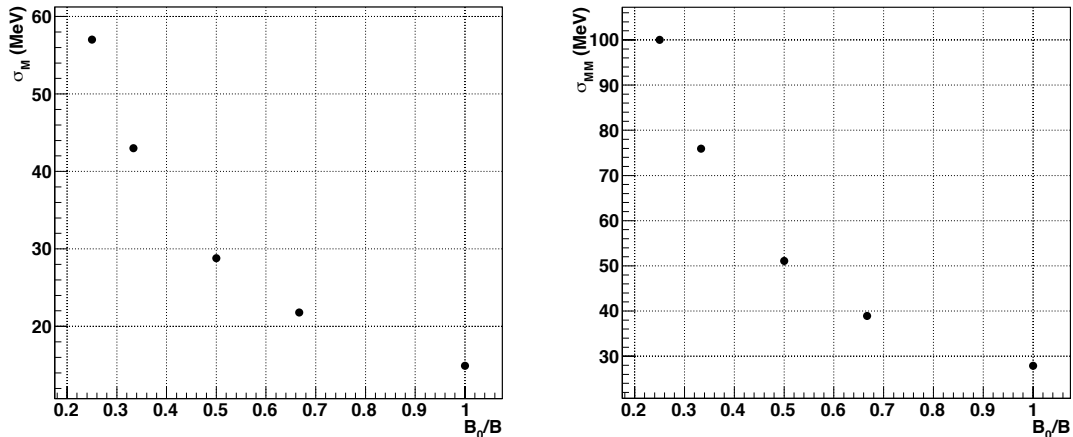


FIG. 19: Left:  $e^+e^-$  measurement, reconstructed  $J/\psi$  mass resolution as a function of the CLAS12 toroidal field intensity (normalized to the maximum possible value). Right: resolution on the missing mass on the  $e^+e^-$  pair as a function of the CLAS12 toroidal field intensity.

We also investigated the effect of a magnetic field variation on the quantities reported above. As expected, we observed that there is almost no dependence on the orientation of the CLAS12 toroidal field, given the charge symmetry of the  $e^+e^-$  system. Some results are reported in Fig. 19.

The CLAS12 acceptance, as a function of the  $pJ/\psi$  invariant mass  $W$ , is reported in Fig. 20, for the two measurement strategies outlined below. For both cases, the acceptance shows a smooth increase with  $W$ , with an average value of  $\simeq 13\%$  for the detection of all final state particles ( $\simeq 16\%$  for the detection of the  $e^+e^-$  pair only). We observe that the “dip” at  $W = 4.4$  GeV, at the resonance mass, is due to the fact that resonance production mechanism is characterized by a very different kinematics than the background, in particular for the  $t$  dependence, and, therefore, the corresponding CLAS12 response is different.

We also investigated the effect of a change in the CLAS12 toroidal field, finding a very modest dependence on it. The larger effect comes from inverting the polarity of the field, i.e. having the proton being inbended by the field. In this case, the acceptance for the measure of all the final state particles drops to  $\simeq 9\%$ , while there is no change for the measure of the  $e^+e^-$  pair only.

Finally, the resolution on the  $pJ/\psi$  invariant mass  $W$ , measured as the missing mass on the low-angle scattered electron, is shown in Fig. 21. As pointed above, this quantity depends only on the measurement of the final state electron with the Forward Tagger calorimeter, and it is almost insensitive to the CLAS12 configuration. For  $W = 4.4$  GeV,  $\sigma_W = 5.5$  MeV, in agreement with the previous estimate.

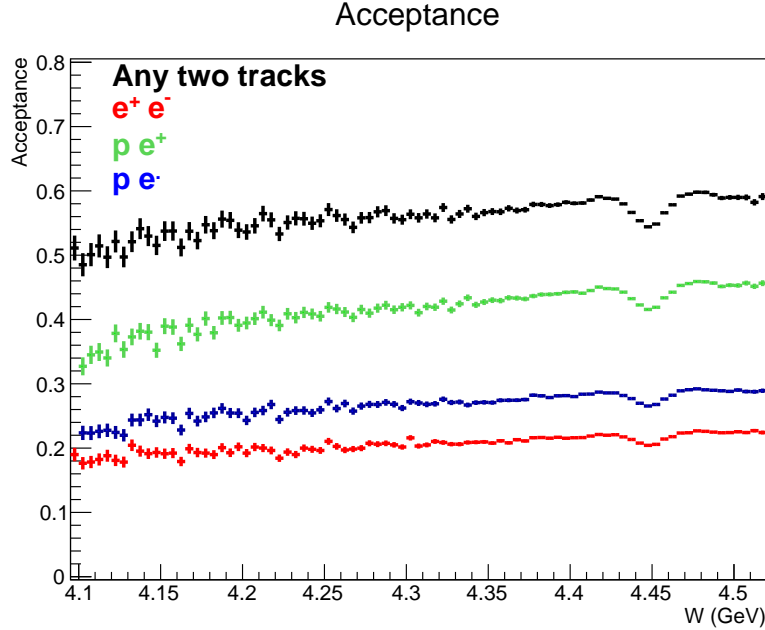


FIG. 20: Detector acceptance as a function of the  $J/\psi p$  invariant mass, for different measurement strategies outlined before, considering only the  $J/\psi \rightarrow e^+e^-$  decay mode. Plots refer to the maximum value of the CLAS12 toroidal field, configured to have positive particles outbending.

### 3. Estimate of the pentaquark yield

As in the previous section, the total number of the events measured by the CLAS12+Forward Tagger for the reaction  $ep \rightarrow P_c \rightarrow J/\psi p e'$ ,  $J/\psi \rightarrow e^+e^-$  was estimated as:

$$N(P_c) = \int \sigma(W) \frac{dL_\gamma}{dW} \epsilon dW \cdot Br(J/\psi \rightarrow e^+e^-) = 0.2 \int \sigma(W) dW \text{ events/nb/MeV/day} \quad (23)$$

where  $\frac{dL_\gamma}{dW} = 7.5 \cdot 10^{28} \text{ events/cm}^2/\text{MeV/s} = 7.5 \cdot 10^{-5} \text{ events/nb/MeV/s}$  is the CLAS12+Forward tagger tagged photon luminosity per  $\Delta W = 1 \text{ MeV}$  bin at the nominal electron-proton luminosity  $L_{ep} = 10^{35} \text{ cm}^{-2} \text{ sec}^{-1}$ , and  $\epsilon$  is the the detection efficiency. We assumed that the three topologies  $pe^+$ ,  $pe^-$ , and  $e^+e^-$ , with two charged particles measured in CLAS12, are considered simultaneously. Hence, the overall efficiency for any two charged particles measured in CLAS12 is about 0.5 at the resonance peak (see Figure 20). Finally, the  $J/\psi \rightarrow e^+e^-$  decay branching fraction (0.06) has to be considered. The pentaquark yield for one day at this luminosity is presented in the Table II for two states and two values of the predicted cross sections shown in Fig. 6, assuming as before  $Br(P_c \rightarrow J/\psi p) = 1\%$ .

These rates are derived assuming only the  $e^+e^-$  decay channel. However, it should be noted that almost all the decay modes of  $J/\psi$  meson involve at least two charged particles, and are thus

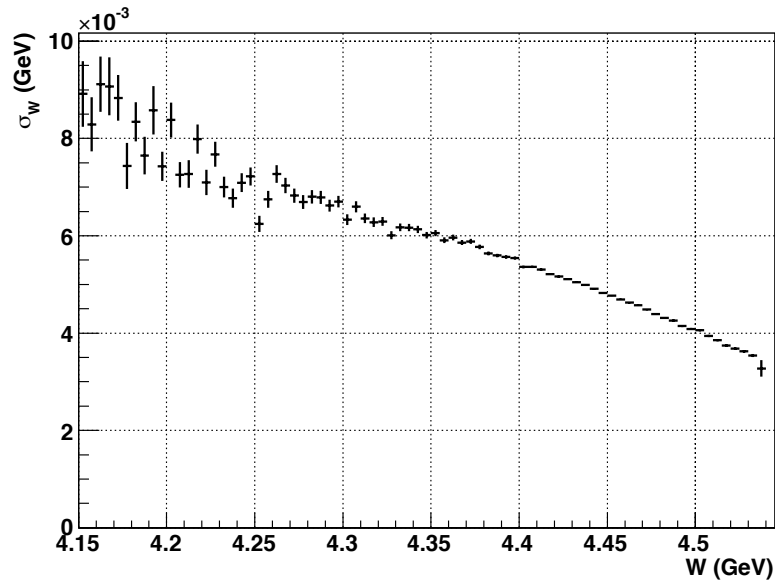


FIG. 21: Resolution on the  $p J/\psi$  invariant mass.

compatible with the experiment trigger setting, requiring the coincidence between an electron cluster in the Forward Tagger calorimeters and two charged tracks in CLAS12. Therefore, by selecting events with one measured proton, and reconstructing the  $J/\psi$  in the missing mass spectrum, it will be possible to enhance the accumulated statistics by a factor of  $1/BR(e^+e^-) \simeq 15$ . In Table II we report the corresponding yield estimates, assuming an average CLAS12 efficiency for the detection of the proton plus any other charged particle from  $J/\psi$  decay of about 0.4 (this number was derived from the  $pe^+e^-$  case discussed before, considering that  $\epsilon(pe^+ + pe^-) \simeq 0.4$ ).

TABLE II: Tagged measurement: estimated number of detected events per day.

	Number of events/day	Number of events/day - $e'p'$ + one charged track
$P_c(4380)$	10 - 300	130 - 3900
$P_c(4450)$	14 - 440	180 - 5700

## V. TRIGGER REQUIREMENTS AND TRIGGER RATES

As was discussed in the previous Sections, the proposed measurements will not require any changes in run conditions of RG-A (beam energy, CLAS12 torus and solenoid magnet settings, luminosity). The only additional requirement is the inclusion of new trigger conditions for the DAQ. We intend to study  $J/\psi$  photoproduction in untagged and tagged photoproduction modes. In the untagged mode, the scattered electron will not be detected, only the recoil proton and both leptons from  $J/\psi$  decay will be detected in CLAS12 FD. In the tagged case, the scattered electron will be detected in the forward tagger, while recoil proton and/or decay leptons will be detected in CLAS12 FD. There are two categories of final states, with and without an electron and/or a positron in CLAS12 FD. The final states that will have an electron or a positron in CLAS12 FD will be a subset of events recorded using the CLAS12 standard electron trigger. The CLAS12 electron trigger rate has been estimated elsewhere to be  $\simeq 2$  kHz. The exclusive final state in the tagged photoproduction reaction will be part of the MesonX trigger, which is  $\simeq 2.8$  kHz [4]. So, only two final states, one of each mode, untagged and tagged photoproduction, will need a new trigger configuration. In Table III final states of interest, required trigger settings, and the expected trigger rates are presented.

TABLE III: Final states, trigger configurations and trigger rates for proposed studies.

Trigger #	Final state	Trigger setting	Expected trigger rate
1	$e'p'\mu^\pm$	Cluster in FT $\otimes$ 2-charged tracks in CLAS12 FD	4 kHz
2	$p'\mu^+\mu^-$	3-charged tracks in CLAS12 FD	2.5 kHz
3	$e'p'e^\pm$ ( $e'$ ) $e^+e^-$ $p'e^+e^-$	CLAS12 electron trigger	2 kHz
4	$e'p'l^+l^-$	MesonX trigger <sup>a</sup>	2.8 kHz

<sup>a</sup>The MesonX trigger proposed in [4] will be subset of trigger #1.

The details of trigger rate estimates for two new final states, #1 and #2, are below.

$e'p'\mu^\pm$ : for this final state the trigger rate will be dominated by accidental coincidences between the electron clusters in the FT and two charged tracks in CLAS12 FD. The rate of such trigger was estimated in E12-11-005 for three or more charged particles detected in CLAS12 and an electron cluster in the FT from 0.5 GeV to 4.5 GeV. Here we perform the same

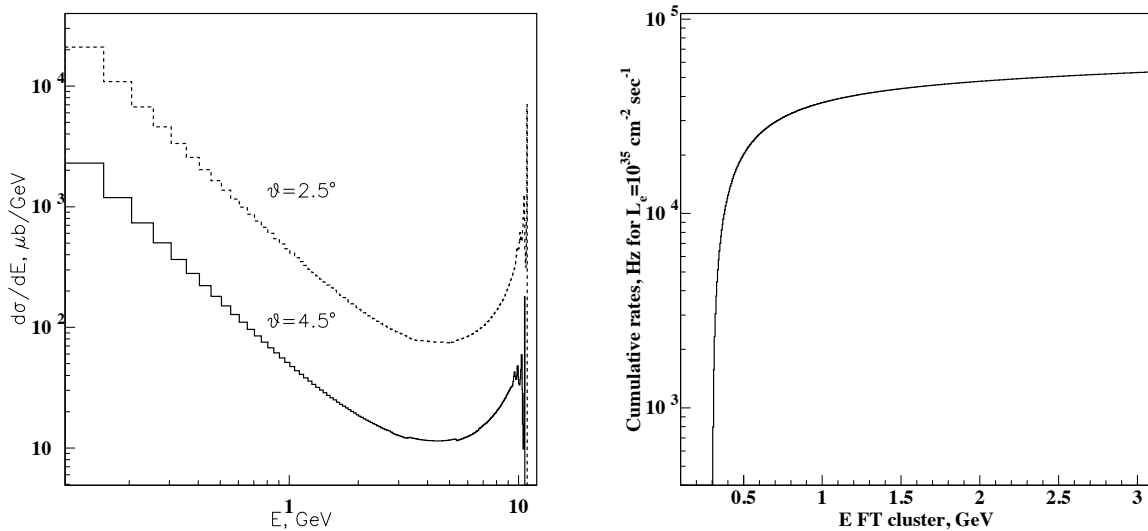


FIG. 22: On the left inclusive electron scattering cross section on hydrogen at 11 GeV. On the right cumulative rate inclusive electrons in FT acceptance region.

exercise but for a coincidence of two or more charged particles detected in CLAS12 FD with 0.3 – 3 GeV electron cluster in the FT (the range of  $J/\psi$  studies).

The electron rates in the FT for hadroproduction in the energies range 0.3 – 3 GeV is  $\sim 4.5$  kHz, see Fig. 7. The rate in the FT is dominated by radiative elastic electrons and by electromagnetic background. The elastic electron scattering cross section was calculated using the code *inclusive* [43] that was validated using CLAS data and used to estimate CLAS12 electron trigger. This code is based on the parametrization of the available world data on inclusive electron scattering and includes radiative effects. In the left graph of Fig. 22, inclusive electron scattering cross section off 5 cm long  $\text{LH}_2$  target is presented for two fixed angles,  $2.5^\circ$  and  $4.5^\circ$ , as function of scattered electron energy. The cross section at small electron energies is on order of  $\sim 10^3 \mu\text{b}/\text{GeV}$  and is dominated by radiative tail. The inclusive electron rates were calculated by integrating the cross section in the angular range of FT. In the right graph of Fig. 22, integrated cumulative rates starting from 0.3 GeV electron energy are shown when electron beam luminosity is  $L = 10^{35} \text{ cm}^{-2} \text{ sec}^{-1}$ . The radiative elastic rate in the energy range up to 3 GeV is  $\simeq 50$  kHz. The background from electromagnetic processes such as Moller scattering, bremsstrahlung, etc. was estimated using GEMC and was found to be  $\sim 180$  kHz, so the total rate of electrons in FT will be

$n_{FT} \simeq 230$  kHz.

The hadronic rate in CLAS12 FD is dominated by photoproduction of two or more charged particles, mostly pions. The main contributions to the total hadronic photoproduction cross section, which is  $100 \mu\text{b}$  above 1 GeV, are from 3-charged particle reactions,  $p\pi^+\pi^-$  and  $p\pi^+\pi^-\pi^0$ , with total cross section of  $\sigma_{3p} \simeq 64 \mu\text{b}$ , and 5-charged particle reaction,  $p\pi^+\pi^-\pi^+\pi^-$ , with  $\sigma_{5p} \simeq 34 \mu\text{b}$  total cross section [44]. In the left graph of Fig. 23, the efficiency of detecting two or more charged particles in CLAS12 FD is plotted as a function of photon energy for these two topologies. The events were simulated assuming exponential  $t$ -dependence,  $e^{5t}$ . The total cross section for two or more charged particles detected in CLAS12 FD is plotted in the right graph of Fig. 23 as a function of photon energy. This cross section was calculated as:

$$\sigma_{det}^2 = \epsilon_{3p} \cdot \sigma_{3p} + \epsilon_{5p} \cdot \sigma_{5p} \quad (24)$$

where  $\epsilon$ s are detection efficiencies for 3- and 5-charged particle reactions. The detected cross section is  $\sim 23 \mu\text{b}$  and is almost independent on the photon energy for  $E_\gamma > 2$  GeV. The total equivalent photon flux for energy region 1.5 GeV to 11 GeV photons is estimated to be  $4800 \mu\text{b}^{-1} \text{sec}^{-1}$  for electron beam luminosity  $L = 10^{35} \text{cm}^{-2} \text{sec}^{-1}$ . Taking the average photoproduction cross section in this region as  $23 \mu\text{b}$  the CLAS12 FD trigger rate with two or more charged particles will be  $n_h = 110$  kHz. The rate of accidental coincidences between CLAS12 FD and FT in  $\delta t = 100$  ns coincidence time window will be:

$$n_{acc} = n_h \cdot n_{FT} \cdot \delta t = 2.53 \text{kHz} \quad (25)$$

Using efficiency estimates in Fig. 23, it is easy to see that the rate of true coincidences between FT electron in the energy range 0.3 – 3 GeV (4.5 kHz) and two or more charged particles in the CLAS12 FD will be:

$$n_{coin} = \frac{4.5 \text{kHz}}{100 \mu\text{b}} \times (0.15 \cdot 34 \mu\text{b} + 0.05 \cdot 64 \mu\text{b}) \simeq 1.2 \text{kHz} \quad (26)$$

bringing the total trigger rate for this final state to about 4 kHz. One should note that this rate is for any two charged tracks triggered in CLAS12 FD.

$p'\mu^+\mu^-$ : in order to estimate the trigger rate for this final state, we simulated the efficiency of the CLAS12 FD for detecting three or more charged particles from the same reactions as above. In Fig. 24 the efficiency and total cross section (as in Eq.24) for detection of three or more

charged particles in CLAS12 FD as a function of photon energy is shown. The trigger rate was calculated using an average total cross section of  $0.9 \mu\text{b}$  and the equivalent photon flux of  $2700 \mu\text{b}$  for  $E_\gamma > 3 \text{ GeV}$ . This resulted to  $< 2500 \text{ Hz}$  trigger rate when three or more charged tracks are required in CLAS12 FD. The same discussion from above on reducing the rate by requiring MIP cuts at the trigger level is applicable here too.

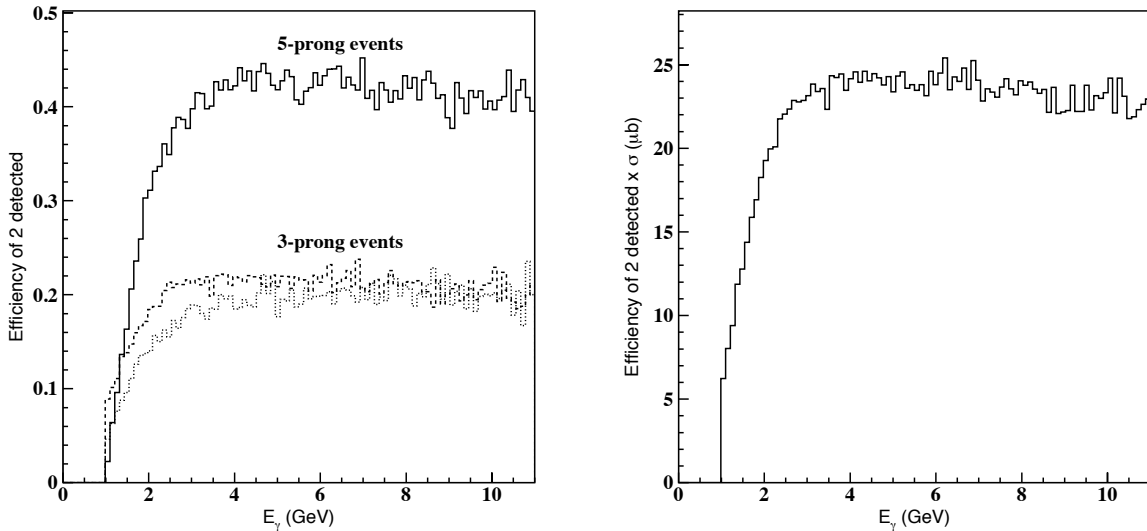


FIG. 23: On the left efficiency of detecting 2-charged particles in CLAS12 FD for different event topologies as a function of incoming photon energy. On the right total cross section of detected events as a function of the photon energy.

Since the new trigger #1 contains the proposed MesonX trigger, the total physics trigger rate will be  $\simeq 8.5 \text{ kHz}$ . Considering a possible trigger purity of  $\sim 50\%$  one would expect  $< 20 \text{ kHz}$  rate to trigger the CLAS12 DAQ. It must be noted that in both final states,  $e'p'\mu^\pm$  and  $p'\mu^+\mu^-$ , the charged tracks will be detected in the ECAL, and one or two of them are the muons, respectively. Therefore the rates of this trigger configurations can be decreased by at least  $\times 2$  for #1, and by  $\times 4$  for #2, requiring a MIP signature for one or two tracks in the ECAL at the trigger level (see discussions in Section IV and Fig. 9).

## VI. EXPECTED RESULTS

In order to estimate expected rates and statistical accuracy of extracting the  $J/\psi$  cross section, we followed the method used in [2]. The  $J/\psi$  production cross section based on the two gluon

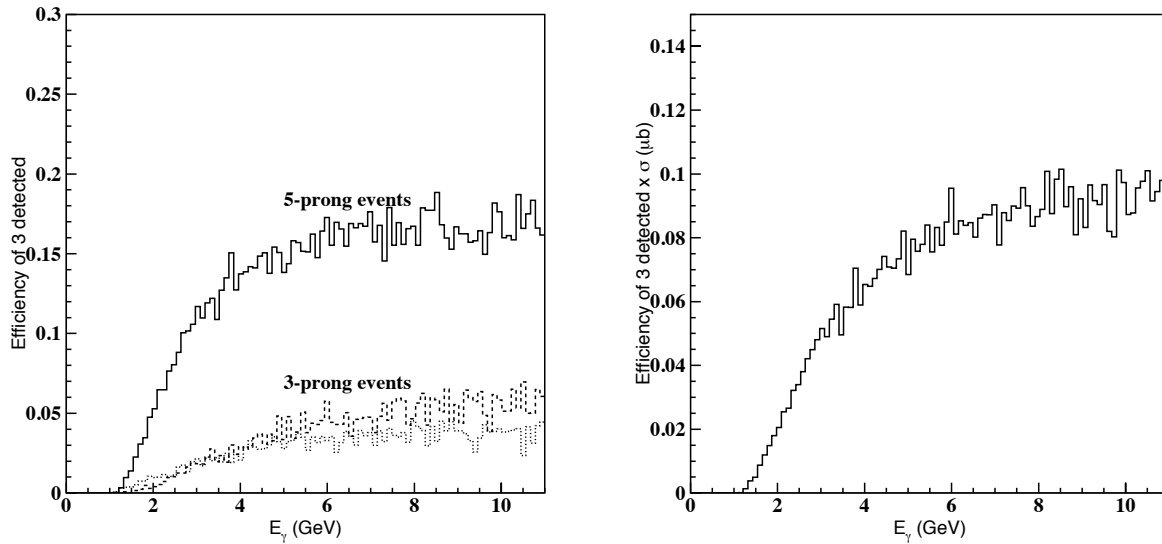


FIG. 24: On the left the efficiency for detecting 3-charged particles in CLAS12 FD for different event topologies as a function of the incoming photon energy. On the right total cross section of detected events as a function of the photon energy.

exchange mechanism was used with exponential  $t$ -dependence as was described in Section III. For pentaquark production the lowest value of the predicted cross section was used. The detector efficiency were obtained from full simulation and reconstruction using GEMC and CoatJava codes. Note that the detector efficiency came out higher by 40% from this the new simulations with correct CLAS12 geometry than what was obtained using the Fast MC code. The luminosity of  $10^{35} \text{ cm}^{-2} \text{ sec}^{-1}$  was assumed. All final states, tagged and untagged photoproduction, were combined in the final results.

Without accounting for pentaquarks, just from the two gluon exchange prediction for cross section, we expect total of 45  $J/\psi$  detected per day in the whole energy range, from threshold to 11 GeV. The rate of pentaquarks for each case, untagged and tagged photoproduction, was given above and is expected to the same order or higher, depending the cross section model and decay branching ratio to  $(J/\psi p)$ . In Fig. 25, the  $J/\psi$  photoproduction total cross section as a function of photon energy is presented with our expected results, red points. The open red crosses when  $P_c(4450)$  was accounted in the cross section calculation, the filled red circles represent expected results if cross section behavior will be according to the two gluon exchange model, model dependence shown by black dashed line. Other black points are existing experimental measurements from SLAC and

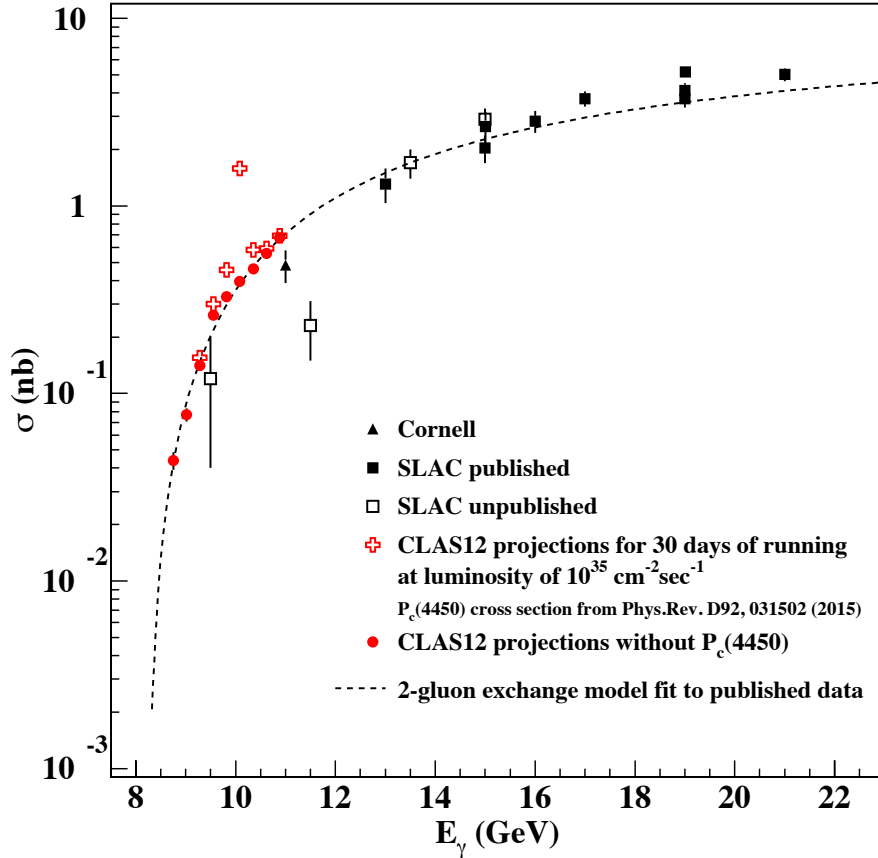


FIG. 25: The total cross section as a function of photon energy for the reaction  $\gamma p \rightarrow p' J/\psi$ . The red points are expected CLAS12 results with (open crosses) and without (filled circles)  $P_c(4450)$ . The cross section based on the two gluon exchange mechanism was used to estimate rates, dashed line. The black points are existing data in this energy region from SLAC and Cornell.

Cornell

## VII. COMPARISON WITH APPROVED JEFFERSON LAB EXPERIMENTS

There are three approved experiments in Halls-A [1], B [2], and C [3] for studying  $J/\psi$  photo- and electroproduction. While no PAC approved proposals, the Hall-D GlueX experiment has already presented  $J/\psi$  measurements from the first engineering run with  $\sim 60$  events, and will produce more results on  $J/\psi$  photoproduction in the near threshold region. In this section we report comparison of this measurements with the others.

The proposed measurement is the extension of E12-12-001. Addition of the  $J/\psi \rightarrow \mu^+\mu^-$  decay mode will double the rate for the untagged photoproduction case. The tagged photoproduction measurements will have 10  $J/\psi$  per day, bringing the total expected rate for  $J/\psi$  detection in CLAS12 to about 45 per day.

The experiment E12-12-006 will use future SoLID detector in Hall-A to measure  $J/\psi$  electroproduction cross section as a function of transferred momentum squared  $t$  and total center-of-mass energy  $W$  in the region  $4.05 \text{ GeV} < W < 4.45 \text{ GeV}$  and  $|t - t_{min}| < 2.5 \text{ GeV}^2$ . With a luminosity of  $10^{37} \text{ N cm}^{-2} \text{ sec}^{-1}$ , the expected rate of  $J/\psi$  is 42/day for 3-prong final state and factor of 3 smaller for the full exclusive final state.

The main goal of the experiment E12-16-007 is the photo-production of the LHCb hidden-charm resonances  $P_c(4380)$  and  $P_c(4450)$  consistent with "pentaquarks". From the proposal addendum we derived that the experiment will detect 100  $P_c(4450)$  events per day assuming 5% branching ratio  $P_c \rightarrow J/\psi + p$ . We have to point out that E12-16-007 used an estimate for the pentaquark cross section which is different from our proposal. Taking this into account we estimated that using the same model used in this proposal E12-16-007 will detect 70  $P_c(4450)$  events per day assuming branching ratio  $BR(P_c \rightarrow J/\psi + p) = 1\%$ . We have to compare this number with 35  $P_c(4450)$  events for the untagged measurements and 14 for the tagged measurements with the decay  $J/\psi \rightarrow e^+e^-$  expected in our measurement. If we will add  $J/\psi \rightarrow \mu^+\mu^-$  decay mode we will end up with 98 CLAS12 events in comparison with 70 events in the E12-16-007 experiment. In addition to that, CLAS12 has almost full angular coverage that will give us the possibility to evaluate the pentaquark quantum numbers in the case this particle will be detected. Hence, other than just confirming the pentaquark existence, CLAS12 can extract the pentaquark properties.

Hall-D has already reported the  $J/\psi$  photoproduction near the threshold. The cross section was not reported yet but the crude estimation gave 5-10  $J/\psi$  mesons detected by the experiment per day at the nominal luminosity in the full energy range. So in total, the CLAS12 expected statistics is at least a factor of 3 bigger than Hall-D has at this moment.

## VIII. SUMMARY

Resolving between models and clarifying the nature of the discovered hidden-charm pentaquark peaks, and possibly searching for similar peaks with other quantum numbers, requires further experimental studies. These states were observed in the decay mode  $J/\psi + p$ . Thus, it is natural to expect that these pentaquarks can be produced in the photoproduction process  $\gamma + p \rightarrow P_c \rightarrow J/\psi + p$  where these states will appear as s-channel resonances at photon energy around 10 GeV. The energies and the luminosities accessible for the CLAS12 detector in Hall-B permit the detailed studies of the production and decay properties of the pentaquark resonances observed by LHCb. For this reason the pentaquark search at Jefferson Laboratory looks extremely attractive.

The peak cross section for  $\gamma + p \rightarrow P_c \rightarrow J/\psi + p$  is likely to reach values that may allow fairly detailed studies of the pentaquarks and a search for other similar states. In particular, it may be realistic to study the decays of the  $P_c$  states into  $J/\psi p \pi$  and  $J/\psi p \pi \pi$ . Such decays should be prominent, if the  $P_c$  states are dominantly a baryo-charmonium, (i.e. a hadro-quarkonium) types [32, 33] composed of  $J/\psi$  and excited nucleon states similar to the known resonances  $N(1440)$  and  $N(1520)$ . The CLAS12 detector has enough acceptance to detect these decay modes. These patterns of  $P_c$  decays would disfavor the molecular models [19–22], where one would expect the natural decay channels into a charmed hyperon and a meson, or from the  $\chi_{c1} p$  complex model [18], where the expected dominant decay is  $P_c(4450) \rightarrow \chi_{c1} + p$ . Obviously, any observation of the  $P_c$  peaks in the  $\gamma p$  cross section would confirm the resonance nature of the peaks and rule out the interpretation [24, 27–29] as ‘accidental’ singularities in the  $\Lambda_b$  decays.

Within the settings of experiments E12-11-005 [4] and E12-12-001 [2], tagged and untagged electroproduction of  $J/\psi$ , search and study of charmed pentaquarks will be done using the CLAS12 detector in Hall-B complementing and extending an experimental program already approved in the other experimental Halls of Jefferson Lab.

- 
- [1] Z.-E. Meziani et al., [https://www.jlab.org/exp\\_prog/proposals/16/PR12-12-006.pdf](https://www.jlab.org/exp_prog/proposals/16/PR12-12-006.pdf).
  - [2] S. Stepanyan et al., [https://www.jlab.org/exp\\_prog/proposals/12/PR12-12-001.pdf](https://www.jlab.org/exp_prog/proposals/12/PR12-12-001.pdf).
  - [3] Z.-E. Meziani et al., [https://www.jlab.org/exp\\_prog/proposals/16/PR12-16-007.pdf](https://www.jlab.org/exp_prog/proposals/16/PR12-16-007.pdf).
  - [4] M. Battaglieri et al., [https://www.jlab.org/exp\\_prog/proposals/12/PR12-11-0015.pdf](https://www.jlab.org/exp_prog/proposals/12/PR12-11-0015.pdf).
  - [5] R. Aaij *et al.* [LHCb Collaboration], Phys. Rev. Lett. **115**, 072001 (2015), arXiv:1507.03414 [hep-ex].
  - [6] M. Binkeley et al., Phys. Rev. Lett. **48** 73 (1982).  
B. H. Denby et al., Phys. Rev. Lett. **52** 795 (1984).

- M. D. Sokoloff et al., Phys. Rev. Lett. **57** 3003 (1986).
- P. L. Frabetti et al., Phys. Lett. **B316** 197 (1993).
- S. Aid et al., Nucl. Phys. **B472** 3 (1996).
- J. Breitweg et al., Z. Phys. **C76** 599 (1997).
- [7] U. Camerini et al., Phys. Rev. Lett. **35**, 483 (1975).  
R. L. Anderson, SLAC-PUB-1471 (1975).
- [8] B. Gittelman et al., Phys. Rev. Lett. **35**, 1616 (1975).
- [9] V. D. Barger and R. J. N. Phillips, Phys. Lett. **B 58**, 433 (1975).
- [10] S.J. Brodsky, E. Chudakov, P. Hoyer, J.M. Laget, Phys. Lett. B **498** , 23 (2001).
- [11] S.J. Brodsky, G.F. de Teramond, I.A. Schmidt, Phys. Rev. Lett. **64** (1990) 1924.
- [12] A. Sibirtsev, S. Krewald, and A. W. Thomas, J. Phys. **G30**, 1427?1444 (2004).
- [13] D. Kharzeev et al., Eur. Phys. J. **C 9**, 459?462 (1999).
- [14] D. Kharzaeev, arXiv:nucl-th/9601029 (1996).
- [15] X. Ji, Phys. Rev. Lett. **74**, 1071 (1995)
- [16] V. Kubarovsky and M.B. Voloshin, Phys.Rev. D **92** (2015) 3, 031502, arXiv:1508.00888 [hep-ph].
- [17] Michael I. Eides, Victor Yu. Petrov, and Maxim V. Polyakov, Phys. Rev. D **93**, 054039 (2016), arXiv:1512.00426 [hep-ph].
- [18] U. G. Meißner and J. A. Oller, Phys. Lett. B **751**, 59 (2015), arXiv:1507.07478 [hep-ph].
- [19] R. Chen, X. Liu, X. Q. Li and S. L. Zhu, Phys. Rev. Lett. **115**, no. 13, 132002 (2015), arXiv:1507.03704 [hep-ph].
- [20] H. X. Chen, W. Chen, X. Liu, T. G. Steele and S. L. Zhu, Phys. Rev. Lett. **115**, no. 17, 172001 (2015), arXiv:1507.03717 [hep-ph].
- [21] L. Roca, J. Nieves and E. Oset, Phys. Rev. D **92**, no. 9, 094003 (2015), arXiv:1507.04249 [hep-ph].
- [22] J. He, Phys. Lett. B **753**, 547 (2016), arXiv:1507.05200 [hep-ph].
- [23] L. Maiani, A. D. Polosa and V. Riquer, Phys. Lett. B **749**, 289 (2015), arXiv:1507.04980 [hep-ph].
- [24] V. V. Anisovich, M. A. Matveev, J. Nyiri, A. V. Sarantsev and A. N. Semenova, arXiv:1507.07652 [hep-ph].
- [25] A. Mironov and A. Morozov, JETP Lett. **102**, no. 5, 271 (2015), arXiv:1507.04694 [hep-ph].
- [26] R. F. Lebed, Phys. Lett. B **749**, 454 (2015), arXiv:1507.05867 [hep-ph].
- [27] F. K. Guo, U. G. Meißner, W. Wang and Z. Yang, Phys. Rev. D **92**, no. 7, 071502 (2015), arXiv:1507.04950 [hep-ph].
- [28] X. H. Liu, Q. Wang and Q. Zhao, Phys. Lett. B **757**, 231 (2016), arXiv:1507.05359 [hep-ph].
- [29] M. Mikhasenko, arXiv:1507.06552 [hep-ph].
- [30] Q. Wang, X. H. Liu and Q. Zhao, Phys. Rev. D **92**, 034022 (2015), arXiv:1508.00339.
- [31] Marek Karliner and Jonathan L. Rosner, Phys. Lett. B **752**, 329 (2016), arXiv:1508.01496.
- [32] M. B. Voloshin, Prog. Part. Nucl. Phys. **61**, 455 (2008) [arXiv:0711.4556 [hep-ph]].
- [33] S. Dubynskiy and M. B. Voloshin, Phys. Lett. B **666**, 344 (2008) [arXiv:0803.2224 [hep-ph]].

- [34] J. Sakurai, Phys. Rev. Lett. 22, p981 (1966).
- [35] V. Kubarovsky and M.B. Voloshin, arXiv:1609.00050.
- [36] K. A. Olive *et al.* [Particle Data Group Collaboration], Chin. Phys. C **38**, 090001 (2014).
- [37] A. N. Hiller Blin *et al.*, Phys. Rev. D **94**, no. 3, 034002 (2016)
- [38] R. Paremuzyan, [https://www.jlab.org/Hall-B/general/thesis/Paremuzyan\\_thesis.pdf](https://www.jlab.org/Hall-B/general/thesis/Paremuzyan_thesis.pdf)
- [39] I. Aznauryan *et al.*, [https://www.jlab.org/exp\\_prog/proposals/07/PR-07-009.pdf](https://www.jlab.org/exp_prog/proposals/07/PR-07-009.pdf)
- [40] M. Davier *et al.*, Phys. Rev. Lett. **21**, 841 (1968).
- [41] K. Abe *et al.*, Phys. Rev. Lett. **53**, 751 (1984).
- [42] A. Celentano [CLAS Collaboration], EPJ Web Conf. **73**, 08004 (2014).
- [43] M. Sargsyan, CLAS Note 1990-007 (1990).
- [44] H.H. Bingham (LBL, Berkeley) *et al.*, Phys.Rev. **D8** (1973) 1277.